FEATURE ARTICLE

Physical Chemistry of Airborne Sea Salt Particles and Their Components

Barbara J. Finlayson-Pitts* and John C. Hemminger†

Department of Chemistry, University of California, Irvine, Irvine, California 92697-2025

Received: August 16, 2000; In Final Form: October 4, 2000

The potential for generation of highly reactive chlorine and bromine atoms from sea salt particles in the troposphere has been recognized for many years. This chemistry is of particular interest because of the complex interactions of halogen atoms with ozone as well as with organics, which can lead to either the formation or destruction of tropospheric ozone, depending on the conditions. While a variety of reactions of tropospherically important gases with sea salt and its major components, NaCl and NaBr, have been identified, the chemical and physical interactions are not well understood on a molecular scale. As a result, quantification of the contribution of sea salt chemistry to the marine boundary layer, as well as in other circumstances where such chemistry may be important, is not yet possible. We discuss here research from the authors' laboratories which is directed to understanding the chemistry of sea salt, NaCl, and NaBr on a molecular level in sufficient detail to provide a firm basis for incorporating this heterogeneous chemistry into atmospheric models. Implications for chemistry in the marine boundary layer and in the Arctic at polar sunrise are discussed, and areas of particular uncertainty highlighted.

Introduction

Over the last few decades, there has been a dramatic increase in research devoted to understanding the fundamental kinetics and mechanisms of atmospheric reactions. It has become clear that all of the traditional areas of chemistry, including physical, organic, inorganic, analytical and biochemistry, are needed to address various problems in this exciting and dynamic field. Furthermore, it is evident that integration of experiments and theory is critical to the development of a full understanding of chemical and physical processes in the atmosphere.

In this article, we focus on one aspect of atmospheric chemistry: reactions of sea salt particles and their components relevant to the atmosphere. In the spirit of a Feature Article, the intent is not an exhaustive review of the burgeoning literature in this area, but rather a summary of recent research carried out in the authors' laboratories. We show how a combination of experimental approaches combined with theory provides new insights into the atmospheric reactions of airborne sea salt particles, and in particular how this integration highlights some new and exciting areas for future research.

Background

Role of Halogens in the Overall Chemistry of the Lower Atmosphere. The major initiators of chain processes in the troposphere have been known for many years to be hydroxyl radicals (OH) during the day, nitrate (NO_3) free radicals at night, and ozone both day and night. The hydroxyl radical is primarily a daytime species because its sources are photolytic, e.g., photolysis of O_3 to give $O(^1D)$ which reacts with water vapor to generate OH, photolysis of HCHO and other aldehydes to give HO_2 which forms OH via the reaction with NO, and photolysis of HONO to give OH directly. Nitrate radicals on the other hand, formed by the reaction of NO_2 with O_3, contribute to chemistry primarily at night because of the rapid photolysis of NO_3 at dawn.[1] Ozone itself initiates chemistry directly and indirectly through its reaction with alkenes; this reaction not only forms free-radical precursors such as HCHO but also generates OH directly through the decomposition of excited Criegee intermediates.[2−4]

However, there is increasing evidence that halogen atoms, particularly chlorine and bromine, may play significant roles in the chemistry of certain regions of the lower atmosphere. Field studies dating back approximately 50 years established that sea salt particles exposed to anthropogenic air pollutants were deficient in chloride and often in bromide as well.[5,6] This observation has since been confirmed many times in a variety of locations around the world.[7−13] The chemistry leading to this halogen deficiency in sea salt particles has generally been attributed to acid ion-exchange reactions, such as that with H_2SO_4 or HNO_3:

$$NaCl_{(s,aq)} + HNO_{3(g)} \rightarrow NaNO_{3(s,aq)} + HCl_{(g)} \qquad (1)$$

HCl does not absorb light with $\lambda > 290$ nm which reaches the troposphere,[1] but it does react with OH to generate highly reactive chlorine atoms,

$$HCl + OH \rightarrow H_2O + Cl \qquad (2)$$

which can react further, ultimately generating Cl_2 via HOCl.[14] The rate constant for this reaction[15] at 298 K is 8.0×10^{-13} cm^3 $molecule^{-1}$ s^{-1}; as a result, at an OH concentration of 1×10^6 radicals cm^{-3}, the estimated lifetime ($\tau = 1/k[OH]$) of HCl

* Phone: (949) 824-7670. Fax: (949) 824-3168. E-mail: bjfinlay@uci.edu.
† Phone: (949) 824-6020. Fax (949) 824-3168. E-mail: jchemmin@uci.edu.

10.1021/jp002968n CCC: $19.00
Published on Web 11/17/2000

is quite long, ~14 days. Because of its solubility, HCl is also efficiently removed by deposition, in competition with reaction with OH.

While such reactions are undoubtedly significant, particularly in the presence of acids, there are additional potential reactions with gases such as N_2O_5, NO_3, $ClONO_2$, and NO_2, which directly form photochemically active gaseous halogen products:[16−57]

$$NaCl + N_2O_5 \rightarrow NaNO_3 + ClNO_2 \quad (3)$$

$$NaCl + NO_3 \rightarrow NaNO_3 + Cl \quad (4)$$

$$NaCl + ClONO_2 \rightarrow NaNO_3 + Cl_2 \quad (5)$$

$$NaCl + 2NO_2 \rightarrow NaNO_3 + ClNO \quad (6)$$

All of the stable gaseous products (and the corresponding bromine species formed in the NaBr reactions) absorb light above 290 nm and dissociate to highly reactive halogen atoms. Once formed, Cl can react not only with O_3 as in the stratosphere

$$Cl + O_3 \rightarrow ClO + O_2 \quad (7)$$

but also with organics, which are plentiful in the troposphere:

$$Cl + C_2H_6 \rightarrow HCl + C_2H_5 \quad (8)$$

A similar reaction of OH with organics occurs during the day, generating H_2O rather than HCl. The alkyl radical formed in reactions such as (8) then reacts with O_2 to generate a peroxy alkyl radical (RO_2), that can oxidize NO to NO_2:

$$RO_2 + NO \rightarrow RO + NO_2 \quad (9)$$

The subsequent photolysis of NO_2 generates O_3:

$$NO_2 + h\nu \rightarrow NO + O(^3P) \quad (10)$$

$$O(^3P) + O_2 \xrightarrow{M} O_3 \quad (11)$$

In short, the generation of chlorine atoms in the lower atmosphere can lead either to ozone destruction or to ozone formation, depending on the particular atmospheric conditions.

Bromine atoms also react with O_3

$$Br + O_3 \rightarrow BrO + O_2 \quad (12)$$

but are less reactive than chlorine atoms toward many organics. For example, the reactions with alkanes are sufficiently slow that they are negligible in the atmosphere.[58,59] However, the reactions with some organics such as HCHO are sufficiently fast[15] to be important under atmospheric conditions:

$$Br + HCHO \rightarrow HBr + CHO \quad (13)$$

For example, ozone destruction at the earth's surface is well-known to occur in the Arctic at polar sunrise.[60−62] It is clear that this loss is associated with gas phase bromine chemistry, with recycling of bromine via heterogeneous reactions that are not at present totally understood. Although chlorine chemistry also occurs during these ozone depletion episodes,[63−69] as discussed in detail below, it is much less important than the molar ratio of chlorine to bromine in unreacted sea salt (~650:1) would imply.

In short, if reactions of sea salt liberate chlorine and/or bromine atoms, there is a potential for them to contribute to the chemistry of the lower atmosphere, particularly the marine boundary layer. Shaw[70] reported the transport of sea salt particles as much as 900 km inland in Alaska. There are also some instances of transport of sea salt into the upper troposphere,[71] and, during eruptions of alkaline volcanoes such as El Chichon, into the stratosphere as well.[72,73] In addition to sea salt, there are some other situations where salt is found in high concentrations in particles. For example, the plumes from burning of the oil wells in Kuwait contained high salt concentrations due to the saltwater mixed in with the oil.[74−81] In addition, recent observations of BrO near the Dead Sea suggest the importance of salt chemistry in the vicinity of saline dry lake beds.[82] Thus, the chemistry which is the focus of this article is relevant to a number of situations found in the atmosphere.

Sources and Forms of Particulate Halogens in the Lower Atmosphere. Sea salt represents a very large source of halogens in the lower atmosphere.[12,83] Wave action generates small airborne droplets of seawater in the marine boundary layer.[84−88] As these droplets are transported, water can evaporate, leaving either small concentrated aqueous solutions of seawater or, at sufficiently low relative humidities, small crystalline particles. The deliquescence point of NaCl and sea salt at 298 K is 75% relative humidity.[89−96] However, there is a hysteresis as the particles are dried, so that the effluorescence points occur at much smaller relative humidities. For NaCl, for example, it is ~40%. This means that in the marine boundary layer where the relative humidity is high, the particles will be aqueous. However, when they are transported to higher altitudes or inland where the relative humidities are lower, they can crystallize to form solid particles.

Given this background, there are a number of questions regarding the chemistry of salt particles which need to be addressed in order to understand their contributions to atmospheric processes:

1. What are the known gas−salt reactions and which are likely to be most important in the atmosphere?

2. How does water affect these reactions? This includes both water as a solvent when the particles are above their deliquescence points, as well as water adsorbed on the crystalline salts at lower relative humidities. In addition, water can be trapped in occlusions between particles and play a role in the uptake and reactions of gases.

3. How do the reactions of concentrated aqueous sea salt particles compare to those of the solid salts, particularly the salts which hold surface-adsorbed water?

4. Why is bromine chemistry so enhanced relative to chlorine chemistry under some conditions?

We shall address these issues in this article, in the context of recent findings from the laboratories of the authors.

Reactions of Solid NaCl Relevant to the Troposphere

The reactions of solid powders of NaCl have been the most extensively studied, particularly those with HNO_3, N_2O_5, NO_2/N_2O_4, NO_3, and $ClONO_2$. Despite what might appear at first glance to be relatively simple reactions, the reported kinetics of these gas−solid reactions are often in disagreement by an order of magnitude or more. Table 1, for example, summarizes some of the reported reaction probabilities for these gases with NaCl. Where multiple measurements have been made using different techniques, disagreement by several orders of magnitude is the norm, rather than the exception.

The lack of agreement in the reaction kinetics for what appear, at least stoichiometrically, to be quite straightforward reactions highlights complexities at the molecular level. As discussed

TABLE 1: Reported Reaction Probabilities for the Reactions of Gaseous Oxides of Nitrogen with Solid NaCl at Room Temperature, the Techniques Used, the Type of Salt Sample, and Typical Concentrations[a] of the Gases in Polluted Coastal Regions

HNO_3 (5 ppb)	N_2O_5 (1 ppb)	NO_3(100 ppt)	NO_2/N_2O_4 (50/6 × 10^{-7} ppb)	$ClONO_2$ (5 ppt)
$(1.3 \pm 0.6) \times 10^{-3}$ (XPS; single crystal, zero product coverage extrapolation)[56]	$>2.5 \times 10^{-3}$ (flow system; powders)[27]	$(4.6 \pm 0.4) \times 10^{-2}$ (Knudsen cell; powders and spray-deposited)[168,169]	$(1.3 \pm 0.6) \times 10^{-4}$ [c] (DRIFTS; powders[37]	(0.23 ± 0.06) (Knudsen cell; powders, spray-deposited and single crystals)[170]
$(1.3 \pm 0.4) \times 10^{-2}$ (flow tube; powders)[126]	$(5 \pm 2) \times 10^{-4}$ (Knudsen cell; powders, spray-deposited salt and single crystal)[42]		$(1.3 \pm 0.3) \times 10^{-6}$ [c] (FTIR; single crystals)[49]	$(4.6 \pm 3.0) \times 10^{-3}$ (flow system; powders)[34]
$(1.4 \pm 0.6) \times 10^{-2}$ (Knudsen cell; powders)[44]	$<1.0 \times 10^{-4}$ (flow tube; powders)[126]		$\sim 10^{-7}$ [d] (Knudsen cell; powders)[171]	
$(2.0 \pm 0.1) \times 10^{-2}$ (Knudsen cell; powders, spray-deposited and single crystals)[40,42]	1×10^{-3} (NaCl coated denuder) [33]			
$(0.9-9) \times 10^{-4}$ [b] (flow tube; powders, thin films)[55]				

[a] From ref 1 except for $ClONO_2$ which is a model-calculated value from ref 135. The N_2O_4 is calculated from the NO_2 concentration and the equilibrium constant[15] for the $2NO_2 \leftrightarrow N_2O_4$ reaction. [b] Observed to depend on the concentration of HNO_3 and water vapor; range cited is for HNO_3 from 7×10^{13} to 6×10^{11} cm^{-3} without added water.[55] [c] Assuming N_2O_4 is the reactant; Peters and Ewing[49] observed that the reaction probability increased by up to several orders of magnitude in the presence of water vapor. [d] Preliminary value assuming NO_2 is the reactant.[170]

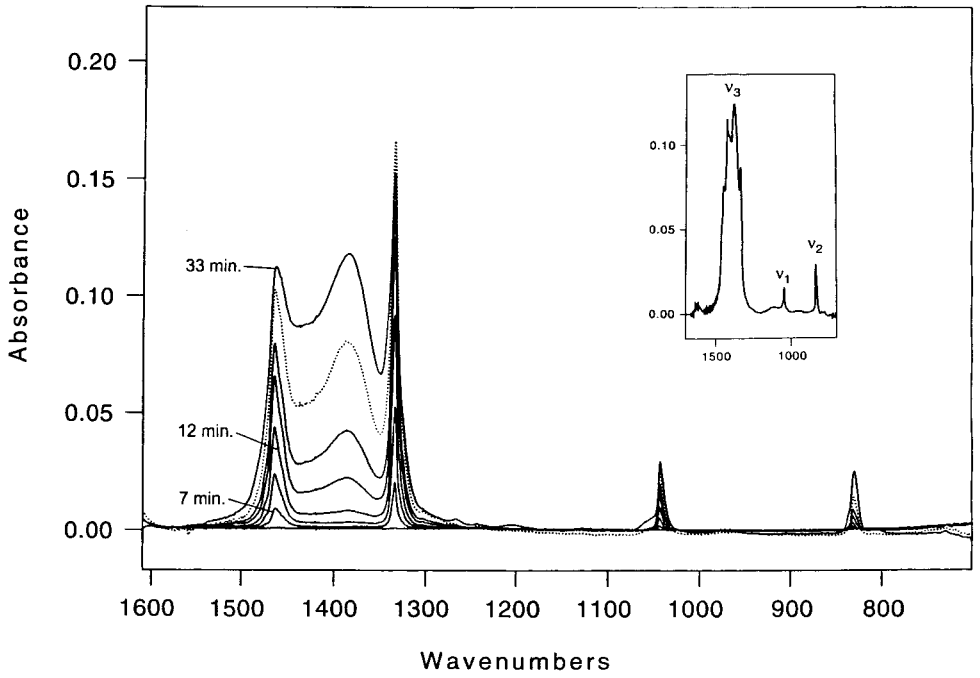

Figure 1. DRIFTS spectra during the reaction of N_2O_5 (5×10^{13} molecules cm^{-3}) with solid NaCl at room temperature. The dotted line is from the reaction of HNO_3 (1.3×10^{14} molecules cm^{-3} for 7 min) with NaCl, demonstrating that the same infrared bands are formed. Inset shows a spectrum of a 0.1% mixture of $NaNO_3$ and NaCl (adapted from Vogt et al., 1994).[38]

below, much of this complexity comes from the effects of water on the salt surface, and in some cases, trapped between particles. In turn, the surface water is associated with steps, edges, and defects on the salt surface. Thus, understanding the kinetics and mechanisms and how to extrapolate to atmospheric conditions requires a detailed knowledge of the molecular scale interactions of both water and the gaseous reactant with the salt surface.

The relative importance of these reactions in the atmosphere is determined by the concentrations of reactant gases, as well as the reaction probabilities. Also shown in Table 1 are some typical concentrations of HNO_3, N_2O_5, NO_3, NO_2/N_2O_4, and $ClONO_2$ measured or calculated to be present in the troposphere under polluted conditions which might be found in coastal urban areas. While the large discrepancies in the reported reaction probabilities preclude making definitive judgments, the combination of the reaction probabilities and concentrations suggest that the most important oxides of nitrogen reactants are expected to be HNO_3, N_2O_5, NO_3, and possibly $ClONO_2$. As discussed earlier, the latter three have the potential to generate highly reactive chlorine atoms more directly than the HNO_3 reaction.

All of the reactions of oxides of nitrogen generate $NaNO_3$, which has been observed as a product by infrared spectroscopy as well as by XPS, SEM-EDS (see below), and AFM.[54] Figure 1, for example, shows a time progression of infrared spectra obtained during the reaction of N_2O_5 with NaCl using diffuse reflectance infrared spectrometry (DRIFTS), and for comparison, one during the reaction of HNO_3 with NaCl.[38] Similar spectra have been observed from the reactions of the other oxides of nitrogen such as NO_2.[37] Bands due to nitrate at 1333 and 1460 cm^{-1}, respectively, increase during the reaction. As seen in

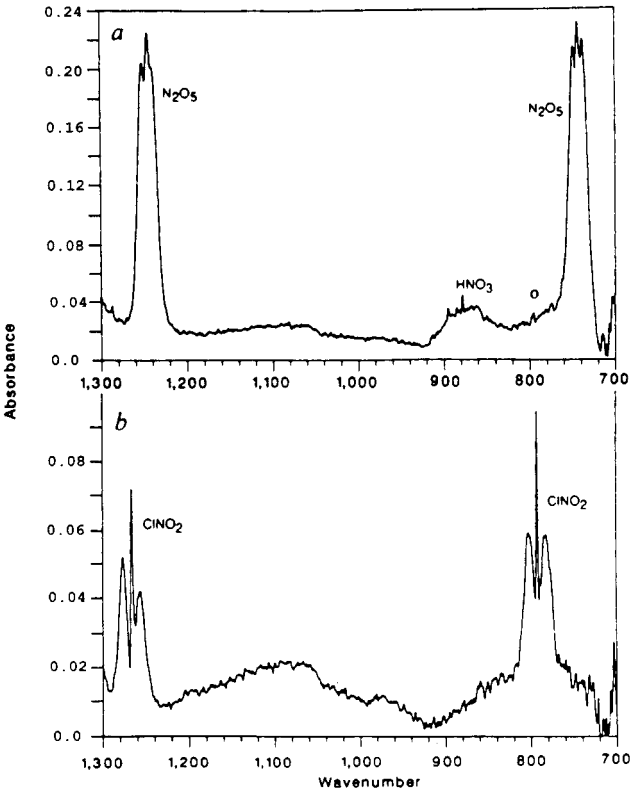

Figure 2. Infrared spectrum of reactants and gas phase products of N_2O_5 with NaCl. Cell had White cell optics with base path of 0.8 m and total path length of 38 m. (a) Before reaction; (b) after 6 ppm N_2O_5 in 1 atm of air had passed over NaCl into the long path cell.[27]

Figure 1, initially there are two narrow bands in the region of the strong ν_3 antisymmetric stretch; as the reaction proceeds, these bands appear to broaden and new bands grow in between. At long reaction times, the peak appears as a very broad band very similar to that observed for bulk crystalline $NaNO_3$ as shown in the inset to Figure 1. That is, while at longer reaction times the product absorptions are clearly due to bulk crystalline $NaNO_3$, the initial spectra observed at low extents of reaction show substantial band splitting. Similar results have been reported by Ewing and co-workers,[49] by Junkermann and Ibusuki[29] and Yoshitake[97] for the reaction of NaCl with oxides of nitrogen. The splitting of the bands was initially assigned[37] to nitrate ions in different environments on the crystal surface. However, Devlin and co-workers[98] suggest that the splitting is due to the transverse and longitudinal modes of dipole active stretching modes of a thin layer of nitrate ions, and Ewing and co-workers[49] propose that the two peaks are due to splitting of the ν_3 degeneracy.

The expected gas phase products of reactions 1 and 3−6 have been observed by FTIR and mass spectrometry. For example, Figure 2 shows the infrared spectrum of the gas phase products from the reaction of N_2O_5 with NaCl. $ClNO_2$ is clearly observed as a product.[27] The gaseous HNO_3 seen in the spectrum may be due to either hydrolysis of N_2O_5 on the surfaces of the vacuum system and/or on the water on the salt surface itself (see below).

Role of Surface-Adsorbed Water on the Reactions of NaCl and Sea Salt

Reactions of Dry Nitric Acid on Defect-Free NaCl Surfaces. Before we discuss the more complex interaction of gas phase reactants with realistic models of sea salt aerosols and particles in the presence of water, it is useful to understand the fundamental processes that occur on structurally well-defined NaCl (single-crystal surfaces) under controlled conditions of adsorbed water. To accomplish this, we have carried out X-ray photoelectron spectroscopy (XPS) and transmission electron microscopy (TEM) studies of the reaction of dry, gas phase HNO_3 with surfaces of single-crystal NaCl(100) samples.[39,43,45,47] As indicated in reaction 1, the interaction of HNO_3 with NaCl leads to the formation of $NaNO_3$ and HCl. The buildup of $NaNO_3$ on the NaCl(100) surface can be followed quantitatively by measuring the XPS signal intensities for N, O and Cl. Figure 3a shows how the surface O, N, and Cl concentrations change as a function of exposure to dry HNO_3 from the gas phase. The N(1s) and O(1s) binding energies measured in these experiments are consistent with the formation of the $NaNO_3$ product. Figure 3a shows that the amount of nitrate product formed on the surface increases initially but then plateaus as the surface

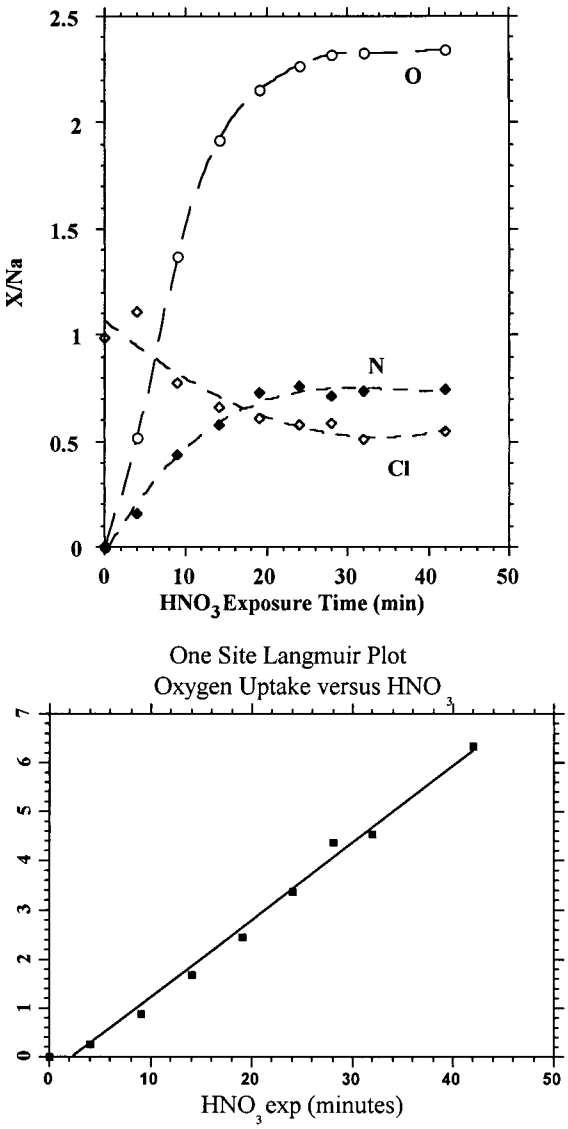

Figure 3. (a, top) O, N, and Cl surface concentrations (relative to Na) as a function of dry HNO_3 exposure time for the NaCl(100) surface; the HNO_3 flux at the surface was equivalent to a gas phase concentration of HNO_3 of 1×10^{11} molecules cm^{-3}. (b, bottom) Plot of $\{-\ln(1 - [O]/[O_{max}])\}$ versus the dry HNO_3 exposure time, where [O] is the oxygen surface concentration shown in Figure 3a, and $[O]_{max}$ is the high exposure saturation value of the oxygen surface concentration shown in Figure 3a. The solid line is a linear least-squares fit to the data, indicating a good fit to a simple, one-site Langmuir adsorption model.[39,43,56]

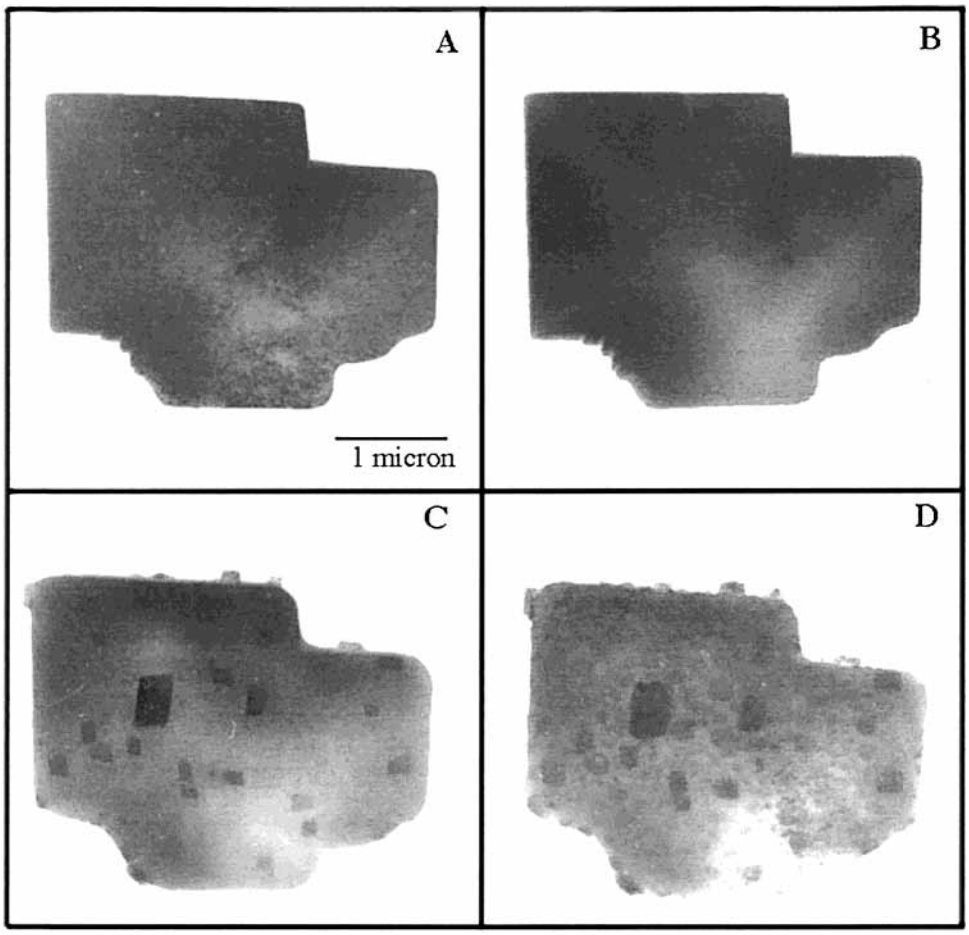

Figure 4. Transmission electron microscope images of a NaCl crystallite: (A) initial crystallite after growth on the TEM grid. (B) after exposure of the sample from (a) to 1.2×10^{15} molecules cm^{-3} HNO_3 for 15 min; (C) after exposure of the sample from (B) to water vapor (<15 Torr); (D) after exposure of the sample from (C) to another sequence of HNO_3 followed by water vapor (adapted from Allen et al., 1996[45] and Hemminger[99]).

becomes covered and passivated with the $NaNO_3$ reaction product. The Langmuir adsorption model provides a simple description of this surface reaction. In this model, it is assumed that a well-defined number of reaction sites exist on the surface prior to exposure to HNO_3 and that as these sites are occupied in a statistical manner, the reaction probability decreases until all of the surface sites are occupied by the reaction product and the reaction probability is zero. This leads to the following relationship between the reaction probability and the surface coverage of product:[56,99,100]

$$\ln\left(1 - \frac{[O]}{[O]_{max}}\right) = -kt \qquad \text{(I)}$$

The surface coverage of the nitrate product is followed using the oxygen surface concentration, [O], from the XPS experiment and $[O]_{max}$ represents the saturation oxygen coverage. k can be combined with the known HNO_3 flux at the surface to calculate the reaction probability at zero coverage. Figure 3b shows the appropriate plot of the oxygen surface coverage as a function of HNO_3 exposure to a NaCl(100) surface from an experiment in which the HNO_3 flux was equivalent to a gas phase concentration of 1×10^{11} molecules cm^{-3}. The reaction probability at zero coverage obtained from the data shown in Figure 3b is $\gamma = (1.3 \pm 0.6) \times 10^{-3}$.

Our XPS experiments demonstrate that the reaction of *dry* HNO_3 with NaCl surfaces is self-limiting. The surface becomes covered with the immobile product of reaction 1, i.e., $NaNO_3$. However, we have also shown that when a surface that has been passivated by reaction with dry HNO_3 is exposed to water vapor, surface reactivity is restored.[43] TEM experiments show that the restoration of surface reactivity occurs because the water exposure results in enhanced ionic mobility on the surface and subsequent recrystallization and phase separation of the $NaNO_3$ passivation layer. As the $NaNO_3$ ultrathin film recrystallizes to form 3-D crystallites, fresh areas of NaCl surface are exposed for subsequent reaction. Figure 4 shows a series of TEM images of a NaCl crystallite before exposure to HNO_3 (Figure 4A), after exposure to HNO_3 (Figure 4B), and after subsequent exposure to water vapor (Figure 4C). There is no apparent change in surface morphology associated with the initial exposure to HNO_3 vapor. However, based on our previous XPS experiments, we know that the surface is covered with a layer of $NaNO_3$. In contrast, the water vapor exposure has resulted in substantial restructuring of the crystallite with the formation of new small crystallites. X-ray fluorescence experiments have allowed us to identify the newly formed crystallites shown in Figure 4C as $NaNO_3$.[45] Our XPS experiments in combination with TEM experiments show that in the absence of water the reaction of HNO_3 with NaCl surfaces is self-limiting. Water can lead to enhanced surface ionic mobility, providing a mechanism for continued steady-state reactivity of the surface. These observations are consistent with the increased mobility of surface ions observed by surface conductance[101] and atomic microscopy[102−105] at relative humidities above ~45%.

Reactions of NaCl Powders. Experiments utilizing NaCl powders to study the reaction with HNO_3 also provide evidence that the initial reaction product is an ultrathin film of $NaNO_3$,

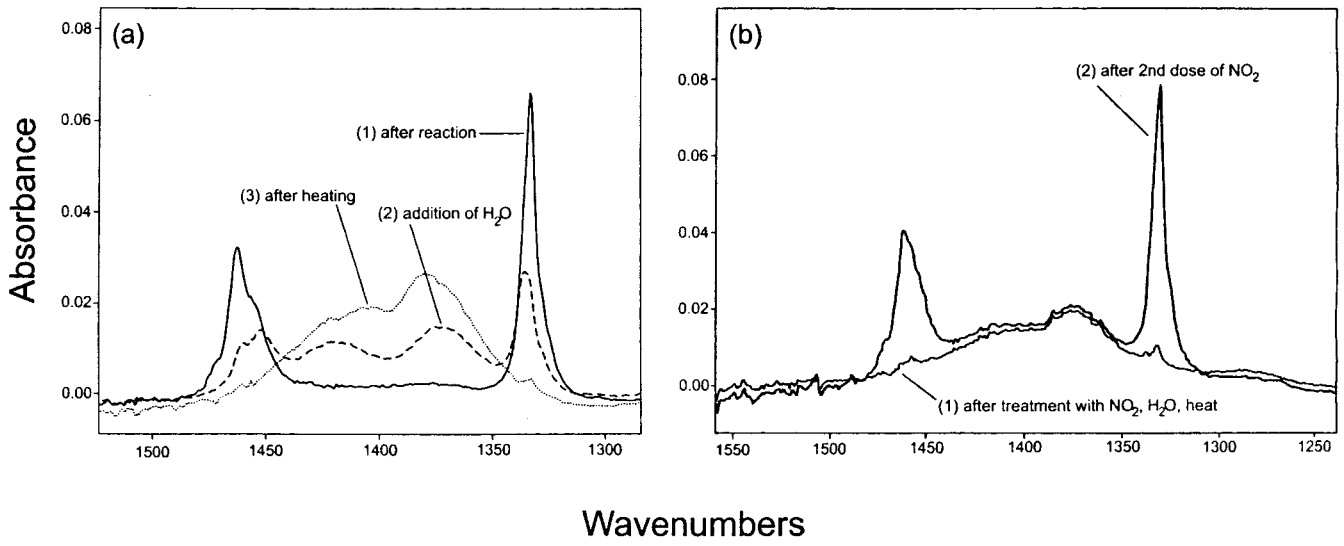

Figure 5. (a) DRIFTS spectra after reaction of (1) 4.5×10^{14} molecules cm^{-3} NO_2 with NaCl for 16 min followed by (2) exposure to 17 mbar water vapor for 2 min. and then (3) heating to 413 K for 1.5 h while pumping; (b) after (1) reaction with NO_2 (5×10^{14} molecules cm^{-3}), then exposure to 7 mbar of H_2O for 25 min. followed by heating at 413 K for 25 min and (2) further reaction with a second dose of gaseous NO_2 (adapted from Vogt et al., 1994).[37]

which recrystallizes to form 3-D crystallites upon postreaction exposure to water vapor. Figure 5a shows DRIFTS spectra in the ν_3 region of NO_3^- (1) after reaction with NO_2 followed by (2) exposure to water vapor and (3) heating and pumping. The nitrate peaks at 1460 and 1333 cm^{-1} (Figure 1) have been replaced by a broad peak between, which is similar to the absorption for crystalline $NaNO_3$ (see inset, Figure 1). This suggests that the surface ions become mobile on exposure to water vapor; upon pumping off the water, the mobile ions recrystallize into small microcrystallites of $NaNO_3$. As a result, the spectrum now resembles that of the bulk crystalline $NaNO_3$. If this is the case, then a fresh surface of NaCl should also have been generated so that additional reaction with NO_2 should generate two nitrate bands in this region, similar to an unreacted NaCl crystal. Figure 5b shows that reacting the salt subsequently with NO_2 does indeed regenerate the 1460 and 1333 cm^{-1} surface nitrate bands. This effect of water exposure is consistent with the results of the XPS and TEM studies previously described.

Key insights regarding the presence of previously unrecognized water on the surface of salt powders and its critical role in determining the reactivity have come out of Knudsen cell studies of the reaction of powders with nitric acid. This is illustrated in Figure 6 which shows Knudsen cell data for the reaction of DNO_3 with NaCl which has been pumped on in the vacuum system, but without prior heating. An interesting feature of the data in Figure 6 is the more rapid initial uptake of DNO_3 when the lid is first opened. There are several possible explanations (or some combination of them) for this spike. One is that there are two types of surface sites on the salt. The initial, more rapid, uptake would then be due to reaction with the first type of site. Once these sites have been completely reacted, the slower reaction on a second type of site continues. For example, small amounts of OH^- have been observed on NaCl.[106−110] Theoretical studies predict that dissociation of water on NaCl to form OH^- occurs at F centers, rather than on steps and edges where molecular adsorption is predicted.[111,112] The initial uptake of HNO_3 would be expected to neutralize these sites. The subsequent uptake may then be due to reaction with chloride.

Another possibility is the presence of water on the surface of the NaCl; on opening the lid, there would be an initially

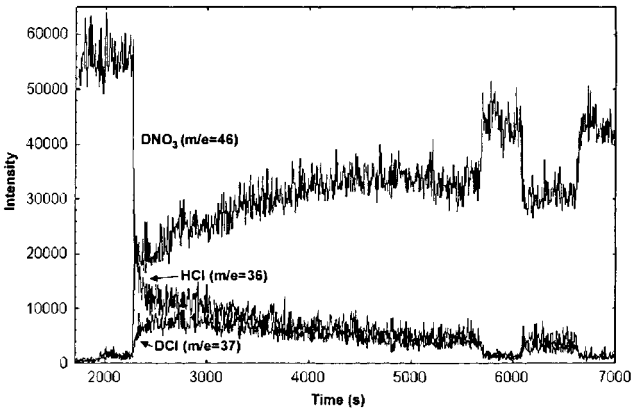

Figure 6. Mass spectrometric signals due to reactant DNO_3 and product HCl in Knudsen cell studies of the reaction of DNO_3 with NaCl powder (1−10 μm) at room temperature. Salt was pumped on for 6 h but not heated prior to reaction (adapted from Beichert and Finlayson-Pitts, 1996).[44]

large uptake of nitric acid due to its solubility in the water layer. This initial uptake would decrease as the aqueous layer approached saturation. Although water is not strongly adsorbed on the NaCl(100) surface under dry conditions at room temperature,[108,109,113−115] water uptake does occur as the relative humidity is increased. For example, Hucher and co-workers[101] measured the surface conductance of NaCl at increasing water vapor concentrations. The conductance was small at relative humidities (RH) less than ∼30% and then increased significantly to 40% RH. Under the latter conditions, there was hypothesized to be a monolayer of physisorbed water on the surface, which has been confirmed by measurements of isotherms for water uptake.[107,116−122] As the relative humidity was increased further, the conductance continued to increase which was attributed to hydration of the Na^+ ions. At the deliquescence relative humidity, dissolution of the surface occurred.

Shindo and co-workers[104,105] used atomic force microscopy to observe the effects of water vapor on the surface of NaCl(100). They reported that motion of the steps on the surface occurred at relative humidities above ∼50%. In addition, and most relevant to the issue of reactions occurring in water on the salt surface, they reported the presence of voids in the natural

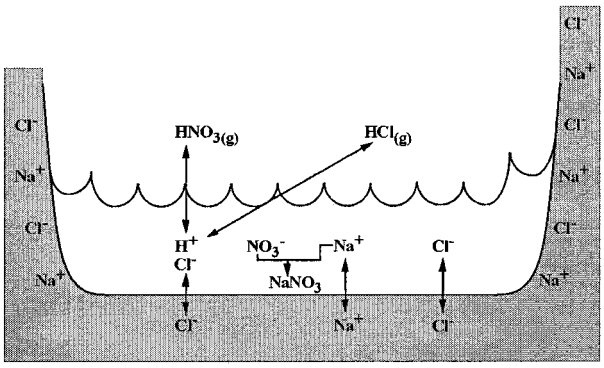

Figure 7. Schematic diagram of chemistry in surface-adsorbed water on NaCl, e.g., in voids on surface.[44]

rock salt crystals used in their studies; these voids were hypothesized to be filled with liquid water which was saturated with salt.

Salmeron and co-workers[102,103] have applied scanning polarization force microscopy to study water uptake on NaCl(100). Between 15 and 35% RH, the apparent height of the step edge peaked above that of adjacent terraces. They attributed this to enhanced water at these step edges. However, as the relative humidity increased above 35%, water was more evenly distributed over the entire surface, in agreement with the observation of increased surface conductance and with previous evidence for a monolayer of water at ~40% RH. Measurements of the surface potential showed that up to ~40% RH preferential dissolution of Na^+ occurs. This is consistent with theoretical studies which predict that adsorption of water at a monatomic step occurs via the interaction of the oxygen with a sodium ion on the edge and one on the terrace below.[112] At higher water vapor concentrations, both the anions and cations dissolve,[103] and the surface ions become much more mobile. This mobility was also seen in the tip carrying material from the step edges as it scanned over them at these relative humidities. In agreement with the work of Shindo and co-workers, motion of the steps was observed at higher relative humidities and at the deliquescence point, all steps disappeared as dissolution of the surface occurred.

In short, there is evidence both for the formation of OH^- at defects on NaCl surfaces as well as for the presence of water adsorbed at steps and edges, as a 2-D layer on the surface and as a 3-D material in voids on the salt surface. Given that the Knudsen cell measurements were carried out under vacuum, water present in voids on the salt surface and/or in occlusions between salt particles[57,93−95,120] appears most likely. In either case, production of HCl would be expected to be delayed relative to uptake of HNO_3. Although the time resolution in these experiments was not sufficient to observe this, a delay in the production of HCl was reported in similar studies by Rossi and co-workers.[40]

Evidence that there is water on the surface that plays a key role in the uptake and reaction of DNO_3 is seen in the products of the reaction (Figure 6). While DCl is generated as expected, substantial amounts of HCl are formed as well. This clearly demonstrates that there must be water on the surface of the salt and that it plays a controlling role in the reaction.

The evidence suggests, then, that there are sites on the NaCl surface which hold water into which the HNO_3 is taken up. Figure 7 is a schematic diagram of the chemistry occurring in the aqueous layer in such sites. It is assumed that the liquid is initially saturated with Na^+ and Cl^-. When the salt is exposed to gaseous HNO_3, it is taken up into the liquid, rapidly reaching saturation. This acidifies the aqueous layer to the point that HCl degasses and is observed as a gas phase product. As HNO_3 continues to be taken up, $NaNO_3$ precipitates out. The thermodynamics of HCl and HNO_3 uptake into water have been described in the literature.[123−125] Application to this system suggests that under typical conditions in these experiments, the pH falls to ~1.7, leading to a constant degassing of HCl and continued uptake of HNO_3.[44]

As we have pointed out previously, the experimentally measured values in the literature for the reaction probability for HNO_3 reacting with NaCl (reaction 1) vary by 2 orders of magnitude (see Table 1). In addition, Davies and Cox[55] and Leu et al.,[126] both report the observation of a dependence of the reaction probability on the HNO_3 pressure. One could explain such a pressure dependence of the reaction probability by assuming a two-site requirement for the dissociative adsorption of HNO_3.[55] However, our XPS experiments (see Figure 3) are more consistent with a simple single site Langmuir model for the dissociative adsorption of HNO_3 on NaCl. The pressure dependence observed by Davies and Cox[55] and Leu et al.[126] is easily explained if we take into account the fact that the steady-state reaction conditions of their experiments require the water induced recrystallization of the $NaNO_3$ reaction product to avoid passivation of the surface. This can be modeled with a two step mechanism as follows:[56]

$$HNO_3(g) + \text{NaCl site} = NO_3^-(ads) + HCl(g) \quad (14)$$

$$NO_3^-(ads) + H_2O(ads) = \text{NaCl site} + NaNO_3(s) \quad (15)$$

where NaCl site represents a surface site that is open for reaction, and NO_3^-(ads) represents a surface nitrate species that is immobile and has blocked the original reactive site. Reaction 15 represents regeneration of the original reactive site in the presence of adsorbed water that acts to increase the nitrate mobility. This simple model provides a description of the HNO_3 pressure dependence that is also consistent with the three major aspects we have learned about the reaction of HNO_3 with solid NaCl: (1) in the absence of water, the dissociative adsorption of HNO_3 on solid NaCl follows a single-site Langmuir model; (2) the initial nitrate formed on the surface blocks subsequent reactions; and (3) water enhances the surface ionic mobility, allowing the recrystallization of the nitrate reaction product and thus opening up sites for further reaction. Using this simple steady state kinetic model, the rate of dissociative adsorption of HNO_3 on NaCl can be written as

$$-\frac{d[HNO_3]}{dt} = \frac{\gamma\bar{c}}{4}[HNO_3]\frac{S}{V} \quad \text{(II)}$$

where $\bar{c}$ is the molecular speed of gas phase HNO_3, S is the NaCl surface area, and V is the reaction cell volume. Similarly, standard expressions can be written for the rate of reactions 14 and 15 as

$$-\frac{d[HNO_3]}{dt} = k_{14}[HNO_3][\text{NaCl site}] \quad \text{(III)}$$

$$\frac{d[NO_3^-(ads)]}{dt} = k_{14}[HNO_3][\text{NaCl site}] - k_{15}[NO_3^-(ads)][H_2O(ads)] \quad \text{(IV)}$$

where k_{14} and k_{15} are the rate constants of reactions 14 and 15 respectively. Using eqns II−IV, one obtains the following

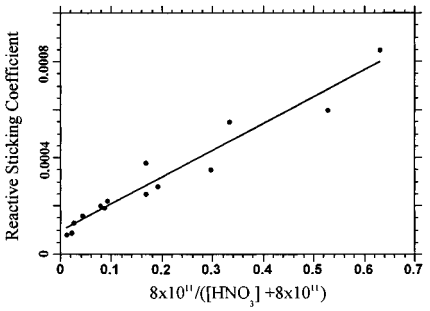

Figure 8. Plot of the reaction probability for HNO_3 on NaCl particles (~0.5 mm diameter) measured by Davies and Cox[55] as a function of $C/([HNO_3] + C$. The constant $C = 8.0 \times 10^{11}$ was chosen to obtain the best linear least-squares fit to the data. This functional form for the behavior of the reaction probability as a function of the HNO_3 gas phase concentration is suggested by the model described in the text.

expression for the reaction probability under steady state conditions:

$$\gamma = k_{14}A\left\{\frac{B[H_2O]}{[HNO_3] + B[H_2O]}\right\} \qquad (V)$$

where A is the total number of surface sites (open + blocked), and $B = 4k_{15}/k_{14}\bar{c}$. Equation V indicates that for reactions run under steady state conditions of constant water content, a plot of γ versus $C/([HNO_3] + C)$ (with C constant at a given water content) should be linear, with a slope equal to $k_{14}A$. Figure 8 shows such a plot of the data from the Davies and Cox study.[55] The fit between the model of reactions 14 and 15 and the pressure-dependent data is quite good.

The maximum value of the reaction probability that can be obtained from the model of reactions 14 and 15 occurs in the limit of high H_2O(ads) concentrations, when the overall steady-state reaction is not limited by the site blocking of NO_3^-(ads). Under such conditions, the maximum value of γ can be obtained from the slope of the plot in Figure 8 as $\gamma_{max} = 1.1 \times 10^{-3}$.

This is in excellent agreement with the value we have measured for the zero coverage reaction probability of dry HNO_3 with NaCl(100) single crystals. This is reasonable since the zero coverage value of the reaction probability should be unaffected by the surface passivation due to the nitrate reaction product and should therefore be comparable to the values of γ measured under steady state conditions when the water-assisted nitrate reorganization is fast and not rate-limiting.

The maximum value of γ just determined is however, still substantially lower than the values reported by Fenter et al.,[40,42] Leu et al.[126] and Beichert and Finlayson-Pitts,[44] which are in good agreement with each other (Table 1). It is probably better to view the reaction on small crystallites in these studies in terms of the previously described picture involving uptake into a liquid like aqueous phase, rather than reactive adsorption onto a solid surface.

Uptake and Reactions of Gases with Synthetic Sea Salt. NaCl is the major component of sea salt and, as a result, has been used extensively in laboratory studies as a surrogate for sea salt. However, sea salt is a complex mixture of inorganics, including a variety of metals and hydrates such as $MgCl_2 \cdot 6H_2O$[127] which have the potential to influence the chemistry. In a Knudsen cell, extensive outgassing of water is observed when sea salt is first placed in the cell, and continues for many hours. In light of the observations of the importance of water on the NaCl powders, reactions of oxides of nitrogen with sea salt should also be controlled by surface-adsorbed water (SAW).

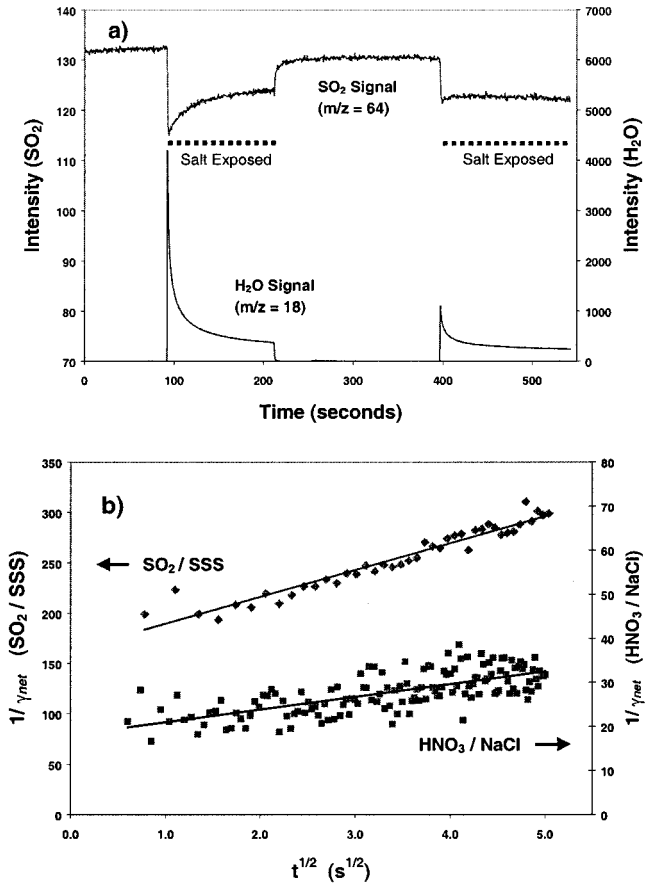

Figure 9. (a) Knudsen cell data of the uptake of SO_2 by synthetic sea salt which had not been heated; (b) plot of $1/\gamma_{net}$ versus $t^{1/2}$ for uptake of SO_2 onto synthetic sea salt, and for HNO_3 onto finely ground NaCl. Both salts had been pumped on but not heated (adapted from Gebel et al., 2000).[128]

Indeed, as discussed in more detail shortly, the results of both Knudsen cell and DRIFTS studies are consistent with this model.

In order to probe water associated with sea salt powders, uptake of SO_2 on synthetic sea salt was studied. Sulfur dioxide is readily taken up into water and dissolves to form $SO_{2(aq)}$, HSO_3^-, and SO_3^{2-}.[1] While a slow reaction of the dissolved S(IV) with carbonates in the salt also occurs, the initial uptake is expected to be controlled primarily by solubility considerations. Figure 9a shows the loss of SO_2, monitored using its parent peak at $m/e = 64$, when the lid of the Knudsen cell is opened to expose the gas to the salt.[128] A rapid initial uptake of SO_2 is observed, followed by a much slower uptake that continues over time scales of hours. This behavior is qualitatively similar to that observed for the uptake of HNO_3 where fast reactions involving chloride in the liquid film may also occur.

The uptake and reaction of gases with liquids is often described by a resistance model.[1,129,130] Under conditions where the uptake is not limited by gas or liquid phase diffusion, the net uptake can be described by eq VI:

$$\frac{1}{\gamma_{net}} = \frac{1}{\alpha} + \frac{1}{\Gamma_{sol} + \Gamma_{rxn}} \qquad (VI)$$

γ_{net} is the measured net uptake coefficient, α is the mass accommodation coefficient, and Γ_{sol} and Γ_{rxn} represent uptake due to dissolution and reaction, respectively, normalized to the rate of gas−surface collisions. If reaction is slow and mass

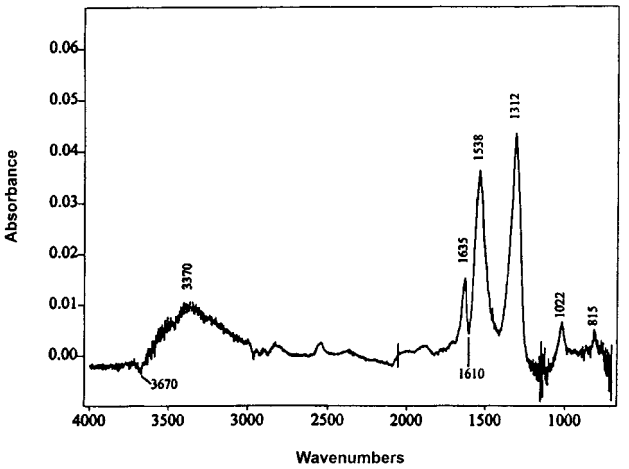

Figure 10. DRIFTS spectra of the reaction of synthetic sea salt with gaseous NO_2 (adapted from Langer et al., 1997).[132]

accommodation is not limiting, then solubility determines the uptake of SO_2. The solubility term is given by eq VII

$$\Gamma_{sol} = \frac{4H^*RT}{\bar{c}}\sqrt{\frac{D_l}{\pi t}} \qquad \text{(VII)}$$

where H^* is the effective Henry's law constant which, in the case of SO_2, depends on the Henry's law constant for physical solubility (H) and on pH:

$$H^* = H\left[1 + \frac{K_1}{[H^+]} + \frac{K_1K_2}{[H^+]^2}\right] \qquad \text{(VIII)}$$

In eq VIII, K_1 and K_2 are the acid dissociation constants for $SO_{2(aq)}$ and HSO_3^-, respectively. Thus, $1/\gamma_{net}$ should vary with $t^{1/2}$ if the uptake of SO_2 onto synthetic sea salt can be described as uptake into an aqueous solution.

Figure 9b shows a plot of $1/\gamma_{net}$ versus $t^{1/2}$ for the initial stages of the uptake of SO_2 onto synthetic sea salt which had been pumped on but not heated. The good agreement with the behavior predicted by eqs VI and VII suggests that this initial "spike" in the uptake can indeed be described as if it were uptake into an aqueous solution. Figure 9b also shows a similar plot for the initial uptake of HNO_3 on finely ground NaCl during experiments similar to those in Figure 6. The linearity of this plot is consistent with an initial rapid uptake of HNO_3 due to dissolution into water on the surface.

The details of Knudsen cell studies of the uptake and reaction of HNO_3 with synthetic sea salt are reported elsewhere.[131] In brief, as expected from the increased amount of water associated with the sea salt, uptake and reaction of HNO_3 is even more rapid than with NaCl. The reaction probability for HNO_3 with salt that had been pumped on but not heated was more than an order of magnitude larger than for NaCl treated in a similar manner. Reaction of DNO_3 with synthetic sea salt which had been heated while pumping for up to 6 h prior to reaction gave HCl as the only significant gas phase product over a period of hours, consistent with the much larger amounts of water associated with sea salt.[131]

DRIFTS studies shed further light on the issue of water in and on synthetic sea salt.[132] Figure 10 shows a typical DRIFTS spectrum for the reaction of NO_2 with synthetic sea salt. Peaks due to NO_3^- at 815 and 1022 cm^{-1} and in the 1300−1500 cm^{-1} range are formed as expected. By comparison to the spectrum from the reaction of NaCl, it can be seen that while nitrate is formed, the peak positions and bandwidths are different for the reaction of synthetic sea salt. Furthermore, new peaks appear at 1635 and 3370 cm^{-1} which, by comparison to spectra obtained by exposing the salt to water vapor, are assigned to surface-adsorbed water. Negative bands at 1610 and 3670 cm^{-1} also appear. Since these are in the region of water absorptions, they could be due to loss of the waters of hydration in the hydrates such as $MgCl_2 \cdot 6H_2O$. Evidence supporting this assignment comes from experiments in which synthetic sea salt was exposed to gas phase D_2O; negative peaks were observed in the same regions, while positive peaks in the 2500 cm^{-1} region and at 1208 cm^{-1} due to D_2O appeared. This suggests that the D_2O not only physisorbed on the surface but also exchanged with some of the water in the crystal structure of the hydrates. Positive bands around 3400 and 1635 cm^{-1} were formed in these experiments, suggesting that some of the water displaced from the hydrates by D_2O remained adsorbed to the salt surfaces. $MgCl_2 \cdot 6H_2O$ was shown to undergo similar reactions as the synthetic sea salt with NO_2, HNO_3, and D_2O.[132]

Weis and Ewing[57] also reported infrared studies of NO_2 with sea salt, in this case suspended as an aerosol in N_2. Formation of particle nitrate as well as gaseous ClNO and HCl was observed. The measured water content of the particles indicated that not only was there water associated with the hydrates in the salt, but water was also present as a liquid possibly trapped in inclusions. Interestingly, the water content increased during the course of the reaction as the product nitrate increased.

In short, synthetic sea salt behaves in some experiments as if it were a saturated liquid salt solution, rather than a solid, with respect to the uptake of gases. Much larger amounts of water are available for this chemistry, compared to the case of NaCl powders. The enhanced amount of water is likely a consequence of the presence of hygroscopic components such as the metal hydrates, as well as water trapped in occlusions between crystals[57,93] as has been observed even in the case of NaCl aerosol particles.[94,95,120]

Reactions of Aqueous Solutions

In the marine boundary layer where sea salt particles are generated, the relative humidity is above the deliquescence point. As a result, sea salt particles consist of concentrated salt solutions, rather than solid particles which would be found in drier areas inland or at higher altitudes. Given the important role of water in the reactions of salt powders discussed above, an intriguing question is whether these concentrated aqueous solutions react in a manner similar to the salts which have water associated with the surface, or whether there is some unique chemistry associated with such aqueous solutions. We briefly describe the results of a combination of experiments, computer kinetics modeling, and molecular dynamics simulations of aqueous sea salt particles which suggest that there are indeed, unique atmospheric reactions of deliquesced sea salt particles.

An aerosol chamber described in detail elsewhere[133] was used to probe the reaction of O_3 as well as OH generated from the photolysis of ozone with NaCl and synthetic sea salt particles. Salt particles were generated using an atomizer, passed through a diffusion drier to generate solid particles, and then flowed into the chamber. Small amounts of CO_2 (~13 ppm) are also present from the diffusion drier. The chamber was filled with air with the desired relative humidity and O_3 then added. Photolysis of the O_3 at 254 nm in this humid system generated OH radicals, and through well-known secondary gas phase chemistry, other species such as HO_2 and H_2O_2 as well, e.g.

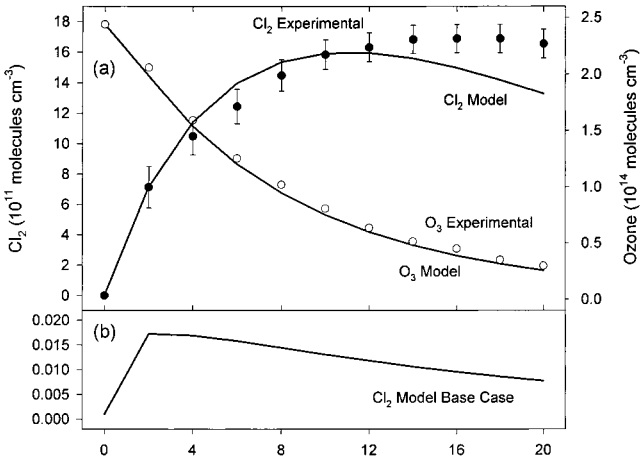

Figure 11. (a) Typical time−concentration profile of O_3 loss and Cl_2 formation. The solid line is the prediction of simulations assuming a self-reaction of a surface OH···Cl^- complex as described in the text; (b) predicted formation of Cl_2 in the experimental system assuming only known gas- and aqueous- phase chemistry; note expanded concentration scale (adapted from Knipping et al., 2000).[136]

$$O_3 + h\nu \rightarrow O(^1D,^3P) + O_2 \quad (16)$$

$$O(^1D) + H_2O \rightarrow 2OH \quad (17)$$

$$OH + O_3 \rightarrow HO_2 + O_2 \quad (18)$$

$$HO_2 + HO_2\ (+M, H_2O) \rightarrow H_2O_2 \quad (19)$$

Figure 11a shows the loss of O_3 measured using differential optical absorption spectrometry in a typical experiment. The only gas phase product observed was Cl_2, also shown in Figure 11a, measured using an atmospheric pressure ionization mass spectrometer (API-MS); ionization occurs at atmospheric pressure via electron transfer from O_2^- formed by a corona discharge in air. The parent ion is isolated in the first quadrupole and then enters a gas collision cell where it is collisionally fragmented. A second scanning quadrupole then identifies the dissociation fragments.

The generation of Cl_2 in this system can be anticipated due to several reaction sequences. In the aqueous phase, oxidation of Cl^- by OH is well-known:[134]

aqueous phase:

$$OH + Cl^- \leftrightarrow HOCl^- \quad (20)$$

$$HOCl^- + H^+ \rightarrow H_2O + Cl \quad (21)$$

$$Cl + Cl^- \rightarrow Cl_2^- \quad (22)$$

$$2Cl_2^- \rightarrow Cl_2 + 2Cl^- \quad (23)$$

The Cl_2 is then released to the gas phase.

Another potential mechanism involves gas phase formation of HOCl, followed by its uptake and reaction in the particles:[14,135]

gas phase:

$$OH + HCl \rightarrow H_2O + Cl \quad (24)$$

$$Cl + O_3 \rightarrow ClO + O_2 \quad (25)$$

$$ClO + HO_2 \rightarrow HOCl + O_2 \quad (26)$$

$$HOCl_{(g)} \rightarrow HOCl_{(aq)} \quad (27)$$

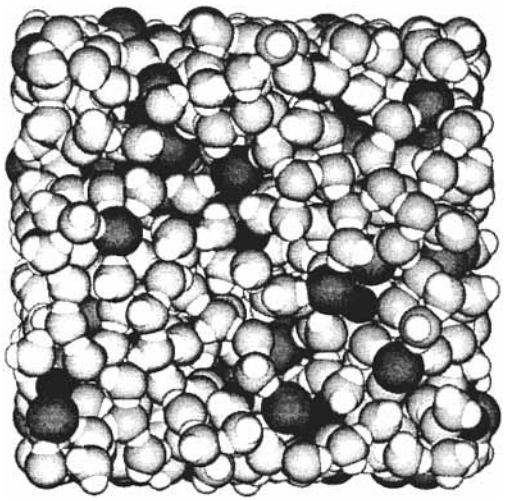

Figure 12. Snapshot of molecular dynamics predictions of typical open surface of a "slab" consisting of 96 NaCl and 864 water molecules. The large medium gray balls are Cl^-, the smaller black balls are Na^+, and the pale gray and white are water (adapted from Knipping et al., 2000).[136]

aqueous phase:

$$HOCl_{(aq)} + Cl^- + H^+ \rightarrow Cl_2 + H_2O \quad (28)$$

$$Cl_{2(aq)} \rightarrow Cl_{2(g)} \quad (29)$$

In order to assess the contributions of such chemistry to the observed Cl_2 formation, a computational kinetics model was developed which included the explicit chemical reactions and diffusion in both the gas and aqueous phases as well as mass accommodation at the particle air−solution interface.[136] The gas phase included 17 individual species and 52 reactions, and the aqueous phase 32 species and 99 reactions. Figure 11b shows the Cl_2 predicted using the full suite of known gas and aqueous phase reactions (note the much smaller concentration scale compared to Figure 11a). The predicted concentrations are seen to be several orders of magnitude smaller than observed. The reason for the small predicted concentrations is that the particles start out approximately neutral, and the CO_2 also buffers the particles: the known reactions summarized above which can generate Cl_2 require acid. As a result, generation of Cl_2 is predicted to be slow.

Molecular dynamics simulations were carried out in order to investigate the possibility of reaction of OH at the particle surface, rather than in the bulk.[136] Figure 12 shows the results of a molecular dynamics simulation of the surface of a cluster of 96 NaCl and 864 water molecules, (the ratio found in a saturated salt solution) using two-dimensional periodic boundary conditions, i.e., an infinite open double surface. A polarizable model[137] was used with an interaction cutoff of 1.2 nm. Long-range interactions were taken into account using the particle-mesh Ewald method.[138] Using a ball of radius 0.17 nm as representative of OH and rolling it across the surface, it was calculated that ~12% of the accessible surface is chloride ion. This is consistent with theoretical studies by Stuart and Berne[139,140] of $Cl^-(H_2O)_n$ clusters (n = 1−499), which show the ready availability of chloride ion at both curved and planar interfaces. Furthermore, quantum chemical calculations show that the complexation energy in the gas phase between OH and Cl^- is ~16.9 kcal mol^{-1} compared to 4.9 kcal mol^{-1} between OH and a water molecule. Hence, not only is the chloride readily available to incoming gases at the surface, but the attractive forces are stronger between the anion and the OH than between

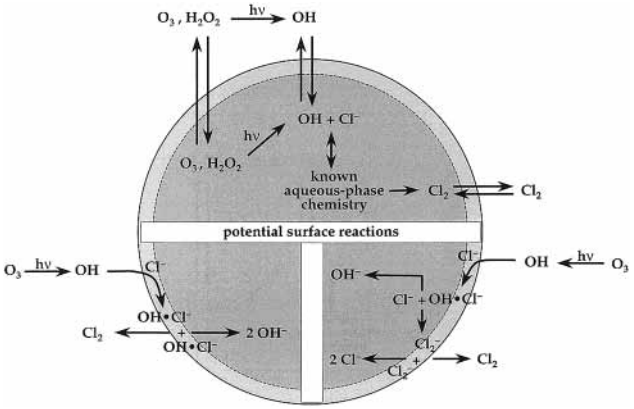

Figure 13. Schematic diagram of potential surface mechanism for production of Cl_2 from the reaction of gas phase OH with chloride ions at the surface of concentrated salt solutions (adapted from Knipping et al., 2000).[136]

water and OH. In short, on a molecular level, interaction of OH with chloride at the surface of the particle is reasonable.

We therefore investigated the possibility that the reactions of a surface complex of OH with chloride might lead to the observed Cl_2 production in our experimental system. While a number of reactions analogous to those in the aqueous phase are plausible, we investigated the self-reaction of an OH···Cl^- complex at the surface as one possibility. This mechanism is summarized in Figure 13. As seen from the solid line in Figure 12a, the experimental observations could be reasonably well matched if it was assumed that the effective rate constant for the self-reactions is the same as that for Cl_2^- (1.8×10^9 L mol^{-1} s^{-1})[141] and that the surface complex decomposes with a rate constant of 1×10^4 s^{-1} in competition with its self-reaction. Another possibility is the formation of Cl_2^- from the OH···Cl^- reaction with Cl^-, followed by its self-reaction in the surface layer. Preliminary molecular dynamics simulations[142] show that Cl_2^- in a concentrated NaCl-water cluster like that in Figure 12 may reside preferentially at the interface, increasing the possibility that its self-reaction in this layer may also play a role in the observed Cl_2 formation.

In summary, it appears from a combination of experiments, computational kinetics modeling, and molecular dynamics simulations that large and polarizable anions may play a significant role at the surfaces of aqueous particles. Not only can their interactions with incoming gases be relatively strong compared to water, but they may have unique chemistry at the interface. Clearly, this is an area that needs much more investigation both experimentally as well as theoretically.

Enhancement of Bromine Chemistry Relative to Chlorine

There is ample evidence that bromine chemistry is responsible for the surface level ozone destruction observed in the Arctic at polar sunrise, and the bulk of the evidence suggests that sea salt is the bromine source. Thus, ozone depletion seems to be associated with air masses advected over sea ice and snow, or over leads (areas of open ocean).[143] While there is evidence that chlorine chemistry is occurring simultaneously,[63] that of bromine is greatly enhanced compared to the Br:Cl molar ratio of 1:650 in seawater. For example, the ratio of integrated bromine atom concentrations to that of bromine during ozone depletion episodes has been estimated[63−69] from the relative rates of decay of selected organics to be $\int[\mathrm{Br}]\,dt/\int[\mathrm{Cl}]\,dt \approx 10^3-10^4$. A major focus of many field, laboratory, and modeling studies has been directed to understanding this very large enhancement of bromine chemistry.

Reaction of Seawater Ice with Ozone. In order to investigate this further, reactions of frozen bulk solutions of the synthetic seawater solution with ozone have also been studied. Solutions with compositions from 28 to 167 g L^{-1} were frozen at −80 °C and O_3 in air passed over the frozen surface which was located in a Teflon reaction chamber. The API-MS sampled from the reaction chamber to probe for production of halogens.

In this case, a reaction was observed in the dark, but only Br_2 was generated. The steady-state Br_2 concentration increased with the initial ozone concentration, with a slight increase in the presence of 254 nm radiation. However, no Cl_2 production was observed either in the dark or under irradiation, in contrast to the reaction of synthetic seawater aerosol particles at room temperature with O_3 irradiated in air.

There are a number of possible contributing factors to the selective production of Br_2 compared to Cl_2 at low temperatures. Ozone is known to readily oxidize bromide in solution, in contrast to chloride ions where the reaction is very slow:[144−146]

$$O_3 + Br^- \rightarrow BrO^- + O_2 \qquad (30)$$

$$BrO^- + H_2O \leftrightarrow HOBr + O_2 \qquad (31)$$

The pK_a of HOBr is 8.8, so that even at a pH of ∼8, typical of seawater, the ratio of HOBr to BrO^- is ∼6. Hence, production of HOBr from the interaction of ozone with seawater is anticipated.

When the temperature of seawater falls, selective crystallization of various components is expected, leaving the remaining liquid with higher concentrations of the remaining species. The eutectic temperature of $NaBr/H_2O$ is 245 K compared to 251 K for $NaCl/H_2O$ and hence in a solution containing the two salts, sodium chloride will crystallize out of solution first, leaving the liquid concentrated in bromide. Molina and coworkers[96] have examined the phase transitions occurring in mixtures of NaCl and water, as well as synthetic sea salt and water. They have shown that when seawater is deposited on the ice pack, the composition of the liquid during cooling favors enhancement of bromide in this layer. Thus, as the solution cools, ice forms first, followed by $NaCl{\cdot}2H_2O$ and then $MgCl_2{\cdot}12H_2O$. Around 240 K, typical of the Arctic in the spring, the chloride ion concentration remaining in the surface film has increased by a factor of ∼11 and the bromide by a factor of ∼38. It is noteworthy that their experiments suggest that the surface films involved will remain liquid under the conditions found in the Arctic spring.

A second major reason for enhancement of gas phase bromine production compared to chlorine lies in the chemistry of bromine and chlorine in solution. Gaseous HOBr is known to react with bromide ion in the aqueous phase, as well as on ice or salt surfaces:[147−152]

$$HOBr + H^+ + Br^- \xrightarrow{\text{aqueous/ice}} Br_2 + H_2O \qquad (32)$$

As discussed above, HOCl undergoes a similar acid-catalyzed reaction with bromide, forming BrCl:[46,148−152]

$$HOBr + H^+ + Cl^- \xrightarrow{\text{aqueous/ice}} BrCl + H_2O \qquad (33)$$

The kinetics of these HOBr reactions, (32) with bromide ion and (33) with chloride, on ice surfaces at lower temperatures[148,149] and in solution at room temperature[147,153] are similar. Thus, the loss process for HOBr formed in reactions (31) and in the gas phase reaction of BrO with HO_2 will depend on the

relative amounts of chloride and bromide ions available for reaction. At molar ratios of Cl^- to Br^- of 650:1 in seawater,[127] or ~200:1 expected for sea salt deposited on the ice pack,[96] the ratio of BrCl to Br_2 might be expected to be in the range of $\sim 10^2 - 10^3$.

The observation that Br_2 is the only significant gas phase product observed in the laboratory studies is consistent with the fact that BrCl is more soluble than Br_2, especially at lower temperatures. The Henry's law constants (H) for BrCl and Br_2 at 298 K are 0.94 and 0.77 M atm^{-1}, respectively;[154] however, using the values of $\Delta H°$ and $\Delta S°$ reported by Bartlett and Margerum,[154] the value of H for BrCl is calculated to increase to 60 M atm^{-1} at 245 K while that for Br_2 only increases to 13 M atm^{-1}. This not only decreases the amount of BrCl released to the gas phase relative to Br_2, but also increases the opportunity for further reaction of BrCl in the aqueous surface film. Bromine chloride is known to react in solution at room temperature with both Br^- and Cl^-:[153]

$$BrCl + Br^- \leftrightarrow Br_2Cl^- \qquad K_{34}(298\ K) = 1.8 \times 10^4\ M^{-1}\ ^{153} \tag{34}$$

$$BrCl + Cl^- \leftrightarrow BrCl_2^- \qquad K_{35}(298\ K) = 6.0\ M^{-1}\ ^{153} \tag{35}$$

Because the surface of the seawater ice under these conditions is thought to be liquid,[96] similar reactions of BrCl might be anticipated in the liquid surface film. If the equilibrium constant K_{34} remains much larger than K_{35} at the lower temperatures (~240 K) characteristic of the springtime Arctic, it more than overcomes the smaller concentrations of bromide ion in seawater which would otherwise favor reaction 35. The Br_2Cl^- formed in reaction 34 decomposes to Br_2 and Cl^-, again favoring bromine formation over chlorine:

$$Br_2Cl^- \leftrightarrow Br_2 + Cl^- \qquad K_{36}(298\ K) = 1.3\ M^{153} \tag{36}$$

In short, the relative amounts of BrCl and Br_2 will be governed by how much of the BrCl initially formed in reaction 33 is emitted to the air and how much undergoes further reactions such as (34) and (35). The fact that Br_2 is the major gaseous product in the laboratory experiments suggests that most of the BrCl undergoes secondary reactions in the ice surface layer to form Br_2, in competition with its release to the gas phase. However, recent ambient air measurements in the Arctic have shown both Br_2 and BrCl to be present, often at similar concentrations.[155] As a result, it appears that under atmospheric conditions, significant quantities of BrCl are released to the gas phase before undergoing secondary reactions in the ice film.

Another contributing factor to the enhancement of bromine chemistry can be inferred from the molecular dynamics simulations (Figure 12) which suggest that the major reason for chloride being readily available at the surface of this large water cluster is the size and polarizability of the anion. This means that the even larger and more polarizable bromide ion should have an even larger presence at the surface of liquids and hence be readily available to react with incoming gases.

Bromine Surface Segregation in Solid Sea Salt Particles. Based on arguments of ion size and polarizability, one might expect Br^- to segregate to the surface of a predominantly NaCl lattice such as would be found in solid sea salt particles. Indeed, using XPS and SEM we have been able to observe segregation of Br to the surface of NaCl single crystals lightly doped with bromide ions.[167] Once again, water is important in this process to provide the ionic mobility required to observe segregation. These experiments involve a NaCl single crystal that was grown from a melt (not from aqueous solution) and which had a bulk Br/Cl ratio of ~0.07. XPS interrogation of a freshly cleaved sample from the single crystal initially shows a surface composition identical to the bulk value, within experimental error. However, following water vapor exposure the surface Br/Cl ratio can be as high as 0.5, i.e., an order of magnitude increase in the Br/Cl ratio at the surface compared to the bulk. Figure 14 shows an SEM image of the surface of a Br doped NaCl(100) sample after water vapor exposure. The light crystallites are NaBr (verified by X-ray fluorescence). The Br has segregated substantially to the surface and has phase-separated to form crystallites of NaBr at the surface.

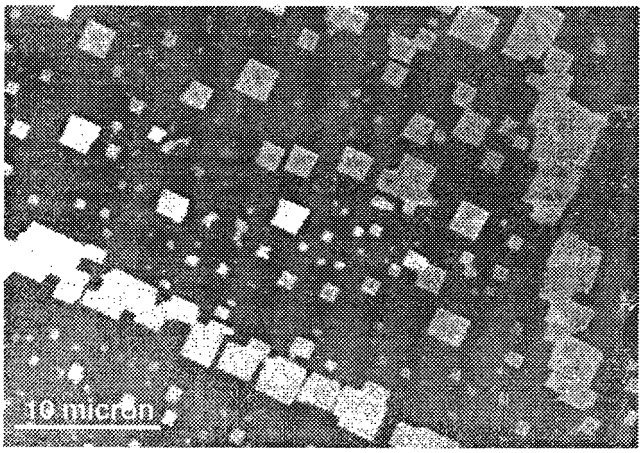

Figure 14. SEM backscattering image of the surface of a bromine doped NaCl(100) surface (bulk composition Br/Cl = 0.07) after exposure to water vapor. The white crystallites are NaBr (confirmed by X-ray fluorescence) that has segregated to the surface (adapted from Ghosal et al., 2000).[167]

Organic Films and Sea Salt Particles

As droplets of seawater are ejected from the ocean to form airborne sea salt particles, they may carry with them some of the organics found at the surface of the ocean. These organics have been hypothesized to play an important role in the chemical and physical processes involved in sea salt in the atmosphere.[156] Such organic films may potentially reduce the rate of evaporation from droplets, inhibit the transport of stable molecules and highly reactive free radicals such as OH between the gas phase and the droplet, and alter the scavenging efficiency with which the particles are scavenged by larger cloud and rain drops.[157] However, there are relatively few experimental studies addressing these issues. For example, some studies[158,159] reported that the uptake of water by NaCl was reduced by an organic coating, although the nature of the organic coating and how it exerts this effect are complex.[159,160] On the other hand, others[161] reported that the addition of a high molecular weight alkane or carboxylic acids to NaCl particles did not significantly alter water absorption by the particles. Oxidation of these films will generate polar moieties (aldehydes, ketones, carboxylic acids) which can alter water uptake as well as radiative properties.[156,162,163]

The lifetime of such organic films on such particles may be shorter than expected based on analogous gas phase reactions. For example, the oxidation by O_3 of monolayers on water of phosphocholines containing one saturated palmitic fatty acid residue (16:0, where the first number represents the number of carbons and the second the number of double bonds) and one oleic acid (18:1) residue, has been shown to be more than an order of magnitude faster than expected from similar gas phase

reactions.[164,165] Furthermore, their surface tension reducing properties are significantly decreased upon oxidation.[164] In a similar vein, Moise and Rudich[166] reported enhanced uptake of gaseous O_3 into liquid unsaturated hydrocarbons compared to densely packed, solidlike monolayers chemisorbed on glass.

Clearly, this is an area in which further experimental studies are needed.

Summary

The reactions of sea salt and its components NaCl and NaBr clearly have the capacity to play a significant role in the atmosphere by acting as precursors to highly reactive chlorine and bromine atoms. Whether such chemistry leads to ozone destruction or formation in the lower atmosphere depends on the particular conditions, e.g., the concentrations of organics and oxides of nitrogen present in the air mass. However, despite what might appear to be relatively simple reactions, there is substantial disagreement on the reaction kinetics and mechanisms of even the simple alkali halide salts. The uncertainties appear to be related in large part to defects, steps and edges on the salt surfaces. These sites are expected to be not only quite reactive, but they also readily take up water and, in the case of surface defects, lead to the formation of OH^- on the surface. Interactions of gases with water on the surface then mimics to a significant extent the uptake and reaction into an aqueous salt solution. Such chemistry appears to be particularly characteristic of finely ground powders. As a result, reactions on such salt powders often do not show surface "saturation" effects, i.e., passivation of the surface after reaction of the top layer, unlike single crystals, in the absence of water, where the reactions cease after reaction of the surface. However, it is still not well understood where on these powders the water is situated nor how to parametrize either the availability of water or the reactivity for a wide variety of NaCl and NaBr reactions.

The production of relatively large amounts of gaseous bromine products compared to chlorine in the reaction of sea salt may be due to a number of contributing factors, the details of which are unfortunately not well understood. For example, the kinetics and mechanisms of reaction of chlorine and bromine compounds in aqueous solution at the low temperatures characteristic of the Arctic at polar sunrise have not been reported. Similarly, the detailed mechanism responsible for surface segregation of bromide in doped NaCl crystals is not well understood.

Clearly, there is a great deal more to be learned on a molecular level regarding the chemistry as well as physical phenomena such as surface segregation effects. Such understanding, however, is critical for quantification of the generation of reactive halogens in the troposphere and the accurate introduction of this chemistry into atmospheric models.

Acknowledgment. The authors are grateful to the National Science Foundation, the Department of Energy and NATO for support of the work described herein. We also thank our collaborators and co-workers in the research described in this article: H. C. Allen, P. Beichert, T. Brauers, D. Dabdub, M. J. Ezell, D. O. De Haan, T. F. Fister, K. L. Foster, J. A. Ganske, M. E. Gebel, R. B. Gerber, S. Ghosal, P. Jungwirth, E. M. Knipping, M. J. Lakin, S. Langer, J. M. Laux, F. E. Livingston, M. Mecartney, K. W. Oum, R. S. Pemberton, A. Shbeeb, J. Stutz, D. J. Tobias, and R. Vogt. We also thank J. N. Pitts, Jr., T. Benter, C. W. Spicer, C. M. Berkowitz, E. G. Chapman, and R. Sander for helpful discussions and M. Molina and R. Sander for providing preprints prior to publication.

References and Notes

(1) Finlayson-Pitts, B. J.; J. N. Pitts, J. *Chemistry of the Upper and Lower Atmosphere—Theory, Experiments, and Applications*; Academic Press: San Diego, CA, 2000.

(2) Atkinson, R.; Aschmann, S. M.; Arey, J.; Shorees, B. *J. Geophys. Res.* **1992**, *97*, 6065.

(3) Atkinson, R. *J. Phys. Chem. Ref. Data* **1997**, *26*, 215.

(4) Paulson, S. E.; Chung, M. Y.; Hasson, A. S. *J. Phys. Chem. A* **1999**, *103*, 8125.

(5) Junge, C. E. *Tellus* **1956**, *8*, 127.

(6) Cicerone, R. J. *Rev. Geophys. Space Phys.* **1981**, *19*, 123.

(7) Moyers, J. L.; Duce, R. A. *J. Geophys. Res.* **1972**, *77*, 5330.

(8) Martens, C. S.; Wesolowski, J. J.; Harriss, R. C.; Kaifer, R. *J. Geophys. Res.* **1973**, *78*, 8778.

(9) Prospero, J. M.; Charlson, R. J.; Mohnen, V.; Jaenicke, R.; Delany, A. C.; Moyers, J.; Zoller, W.; Rahn, K. *Rev. Geophys. Space Phys.* **1983**, *21*, 1607.

(10) Keene, W. C.; Pszenny, A. A. P.; Jacob, D. J.; Duce, R. A.; Galloway, J. N.; Schultz-Tokos, J. J.; Sievering, H.; Boatman, J. F. *Global Biogeochem. Cycles* **1990**, *4*, 407.

(11) Mouri, H.; Okada, K. *Geophys. Res. Lett.* **1993**, *20*, 49.

(12) Graedel, T. E.; Keene, W. C. *Global Biogeochem. Cycles* **1995**, *9*, 47.

(13) Zhuang, H.; Chan, C. K.; Fang, M.; Wexler, A. S. *Atmos. Environ.* **1999**, *33*,

(14) Sander, R. Personal communication.

(15) DeMore, W. B.; Sander, S. P.; Golden, D. M.; Hampson, R. F.; Kurylo, M. J.; Howard, C. J.; Ravishankara, A. R.; Kolb, C. E.; Molina, M. J. "Chemical Kinetics and Photochemical Data for Use in Stratospheric Modeling, Evaluation No. 12,", 1997.

(16) Robbins, R. C.; Cadle, R. D.; Eckhardt, D. L. *J. Meteorol.* **1959**, *16*, 53.

(17) Cadle, R. D.; Robbins, R. C. *Discuss. Faraday Soc.* **1960**, *30*, 155.

(18) Schroeder, W. H.; Urone, P. *Environ. Sci. Technol.* **1974**, *8*, 756.

(19) Finlayson-Pitts, B. J. *Nature* **1983**, *306*, 676.

(20) *Simulation of Atmospheric Photochemistry in the Presence of Solid Airborne Aerosols*; Zetzsch, C., Ed.; VCH Publishers: Weinheim, Germany, 1987; Vol. 104, p 187.

(21) Zetzsch, C.; Pfahler, G.; Behnke, W. *J. Aerosol Sci.* **1988**, *19*, 1203.

(22) Finlayson-Pitts, B. J.; Ezell, M. J.; J. N. Pitts, J. *Nature* **1989**, *337*, 241.

(23) Behnke, W.; Zetzsch, C. *J. Aerosol Sci.* **1989**, *20*, 1167.

(24) *Smog Chamber Investigations of the Influence of NaCl Aerosol on the Concentration of O_3 in a Photosmog System*; Behnke, W., Zetzsch, C., Eds.; Deepak Publishing: New York, 1989; p 519.

(25) Behnke, W.; Zetzsch, C. *J. Aerosol Sci.* **1990**, *21*, S229.

(26) Behnke, W.; Kruger, H.-U.; Scheer, V.; Zetzsch, C. *J. Aerosol Sci.* **1990**, *22*, S609.

(27) Livingston, F. E.; Finlayson-Pitts, B. J. *Geophys. Res. Lett.* **1991**, *18*, 17.

(28) Winkler, T.; Goschnick, J.; Ache, H. J. *J. Aerosol Sci.* **1991**, *22*, S605.

(29) Junkermann, W.; Ibusuki, T. *Atmos. Environ.* **1992**, *26A*, 3099.

(30) Behnke, W.; V, S.; Zetzsch, C. *J. Aerosol Sci.* **1993**, *24*, 5115.

(31) Behnke, W.; Scheer, V.; Zetzsch, C. *J. Aerosol Sci.* **1994**, *S25*, 277.

(32) George, C.; Ponche, J. L.; Mirabel, P. *J. Phys. Chem.* **1994**, *98*, 8780.

(33) Msibi, I. M.; Li, Y.; Shi, J. P.; Harrison, R. M. *J. Atmos. Chem.* **1994**, *18*, 291.

(34) Timonen, R. S.; Chu, L. T.; Leu, M.-T.; Keyser, L. F. *J. Phys. Chem.* **1994**, *98*, 9509.

(35) Zetzsch, C.; Behnke, W. *Ber. Bunsen-Ges. Phys. Chem.* **1992**, *96*, 488.

(36) *Heterogeneous Reactions of Chlorine Compounds*; Zetzsch, C., Behnke, W., Eds.; Springer-Verlag: Berlin, 1993; Vol. 17, p 291.

(37) Vogt, R.; Finlayson-Pitts, B. J. *J. Phys. Chem.* **1994**, *98*, 3747; **1995**, *99*, 13052.

(38) Vogt, R.; Finlayson-Pitts, B. J. *Geophys. Res. Lett.* **1994**, *21*, 2291.

(39) Laux, J. M.; Hemminger, J. C.; Finlayson-Pitts, B. J. *Geophys. Res. Lett.* **1994**, *21*, 1623.

(40) Fenter, F. F.; Caloz, F.; Rossi, M. J. *J. Phys. Chem.* **1994**, *98*, 9801.

(41) Behnke, W.; Scheer, V.; Zetzsch, C. Production of a Photolytic Precursor of Atomic Cl from Aerosols and Cl^- in the Presence of O_3. In *Naturally-Produced Organohalogens*; Grimwall, A., Leer, E. W. B. d., Eds.; Academic Publishers: Dordrecht, 1995; p 375.
(42) Fenter, F. F.; Caloz, F.; Rossi, M. J. *J. Phys. Chem. A* **1996**, *100*, 1008.
(43) Laux, J. M.; Fister, T. F.; Finlayson-Pitts, B. J.; Hemminger, J. C. *J. Phys. Chem.* **1996**, *100*, 19891.
(44) Beichert, P.; Finlayson-Pitts, B. J. *J. Phys. Chem.* **1996**, *100*, 15218.
(45) Allen, H. C.; Laux, J. M.; Vogt, R.; Finlayson-Pitts, B. J.; Hemminger, J. C. *J. Phys. Chem.* **1996**, *100*, 6371.
(46) Abbatt, J. P. D.; Waschewsky, G. C. G. *J. Phys. Chem. A* **1998**, *102*, 3719.
(47) Vogt, R.; Elliott, C.; Allen, H. C.; Laux, J. M.; Hemminger, J. C.; Finlayson-Pitts, B. J. *Atmos. Environ.* **1996**, *30*, 1729.
(48) Karlsson, R.; Ljungstrom, E. *J. Aerosol Sci.* **1995**, *26*, 39.
(49) Peters, S. J.; Ewing, G. E. *J. Phys. Chem.* **1996**, *100*, 14093.
(50) Caloz, F.; Fenter, F. F.; Rossi, M. J. *J. Phys. Chem.* **1996**, *100*, 7494.
(51) Behnke, W.; George, C.; Scheer, V.; Zetzsch, C. *J. Geophys. Res.* **1997**, *102*, 3795.
(52) Schweitzer, F.; Mirabel, P.; George, C. *J. Phys. Chem. A* **1998**, *102*, 3942.
(53) ten Brink, H. M. *J. Aerosol Sci.* **1998**, *29*, 57.
(54) Zangmeister, C. D.; Pemberton, J. E. *J. Phys. Chem. B* **1998**, *102*, 8950.
(55) Davies, J. A.; Cox, R. A. *J. Phys. Chem. A* **1998**, *102*, 7631.
(56) Ghosal, S.; Hemminger, J. C. *J. Phys. Chem. A* **1999**, *103*, 4777.
(57) Weis, D. D.; Ewing, G. E. *J. Phys. Chem. A* **1999**, *103*, 4865.
(58) Wallington, T. J.; Skewes, L.; Siegl, W. O.; Japar, S. M. *Int. J. Chem. Kinet.* **1989**, *21*, 1069.
(59) Barnes, I.; Bastian, V.; Becker, K. H.; Overath, R.; Tong, Z. *Int. J. Chem. Kinet.* **1989**, *21*, 499.
(60) Bottenheim, J. W.; Gallant, A. G.; Brice, K. A. *Geophys. Res. Lett.* **1986**, *13*, 113.
(61) Oltmans, S. J.; Komhyr, W. D. *J. Geophys. Res.* **1986**, *91*, 5229.
(62) Barrie, L. A.; Bottenheim, J. W.; Schnell, R. C.; Crutzen, P. J.; Rasmussen, R. A. *Nature* **1988**, *334*, 138.
(63) Jobson, B. T.; Niki, H.; Yokouchi, Y.; Bottenheim, J.; Hopper, F.; Leaitch, R. *J. Geophys. Res.* **1994**, *99*, 25355.
(64) Yokouchi, Y.; Akimoto, H.; Barrie, L. A.; Bottenheim, J. W.; Anlauf, K.; Jobson, B. T. *J. Geophys. Res.* **1994**, *99*, 25379.
(65) Solberg, S.; Schmidbauer, N.; Semb, A.; Stordal, F.; Hov, O. *J. Atmos. Chem.* **1996**, *23*, 301.
(66) Ariya, P. A.; Jobson, B. T.; Sander, R.; Niki, H.; Harris, G. W.; Hopper, J. F.; Anlauf, K. G. *J. Geophys. Res.* **1998**, *103*, 13.
(67) Ramacher, B.; Rudolph, J.; Koppmann, R. *J. Geophys. Res.* **1999**, *104*, 3633.
(68) Ariya, P. A.; Niki, H.; Harris, G. W.; Anlauf, K. G.; Worthy, D. E. J. *Atmos. Environ.* **1999**, *33*, 931.
(69) Boudries, H.; Bottenheim, J. W. *Geophys. Res. Lett.* **2000**, *27*, 517.
(70) Shaw, G. E. *J. Geophys. Res.* **1991**, *96*, 22369.
(71) Ikegami, M.; Okada, K.; Zaizen, Y.; Makino, Y. *Tellus* **1994**, *46B*, 142.
(72) Woods, D. C.; Chuan, R. L. *Geophys. Res. Lett.* **1983**, *10*, 1041.
(73) Woods, D. C.; Chuna, R. L.; Rose, W. I. *Science* **1985**, *230*, 170.
(74) Ferek, R. J.; Hobbs, P. V.; Herring, J. A.; Laursen, K. K.; Weiss, R. E.; Rasmussen, R. A. *J. Geophys. Res.* **1992**, *97*, 14483.
(75) Cahill, T. A.; Wilkinson, K.; Schnell, R. *J. Geophys. Res.* **1992**, *97*, 14513.
(76) Parungo, F.; Kopcewicz, B.; Nagamoto, C.; Schnell, R.; Sheridan, P.; Zhu, C.; Harris, J. *J. Geophys. Res.* **1992**, *97*, 15867.
(77) Cofer, W. R.; Stevens, R. K.; Winstead, E. L.; Pinto, J. P.; Sebacher, D. I.; Abdulraheem, M. Y.; Al-Sahafi, M.; Mazurek, M. A.; Rasmussen, R. A.; Cahoon, D. R.; Levy, J. S. *J. Geophys. Res.* **1992**, *97*, 14521.
(78) Sheridan, P. J.; Schnell, R. C.; Hofmann, D. J.; Harris, J. M.; Deshler, T. *Geophys. Res. Lett.* **1992**, *19*, 389.
(79) Daum, P. H.; Al-Sunaid, A.; Busness, K. M.; Hales, J. M.; Mazurek, M. *J. Geophys. Res.* **1993**, *98*, 16809.
(80) Lowenthal, D. H.; Borys, R. D.; Rogers, C. F.; Chow, J. C.; Stevens, R. K.; Pinto, J. P.; Ondov, J. M. *Geophys. Res. Lett.* **1993**, *20*, 691.
(81) Stevens, R.; Pinto, J.; Mamane, Y.; Ondov, J.; Abdulraheem, M.; Al-Majed, N.; Sadek, J.; Cofer, W.; Elenson, W.; Kellogg, R. *Water Sci. Technol.* **1993**, *27*, 223.
(82) Hebestreit, K.; Stutz, J.; Rozen, D.; Matveiv, V.; Peleg, M.; Luria, M.; Platt, U. *Science* **1999**, *283*, 55.
(83) Erickson, D. J.; Seuzaret, C.; Keene, W. C.; Gong, S. L. *J. Geophys. Res.* **1999**, *104*, 8347.
(84) Woodcock, A. H. *J. Meteorol.* **1953**, *10*, 362.
(85) Woodcock, A. H. *J. Geophys. Res.* **1972**, *77*, 5316.
(86) Blanchard, D. C. *J. Geophys. Res.* **1985**, *90*, 961.
(87) Gong, S. L.; Barrie, L. A. *J. Geophys. Res.* **1997**, *102*, 3805.
(88) Gong, S. L.; Barrie, L. A.; Prospero, J. M.; Savoie, D. L.; Ayers, G. P.; Blanchet, J.-P.; Spacek, L. *J. Geophys. Res.* **1997**, *102*, 3819.
(89) Twomey, S. *J. Appl. Phys.* **1953**, *24*, 1099.
(90) Orr, C., Jr.; Hurd, F. K.; Corbett, W. J. *J. Colloid Sci.* **1958**, *13*, 472.
(91) Tang, I. N.; Munkelwitz, H. R.; Wang, N. *J. Colloid Interface Sci.* **1986**, *14*, 409.
(92) Cohen, M. D.; Flagan, R. C.; Seinfeld, J. H. *J. Phys. Chem.* **1987**, *91*, 4563.
(93) Tang, I. N.; Tridico, A. C.; Fung, K. H. *J. Geophys. Res.* **1997**, *102*, 23.
(94) Cziczo, D. J.; Nowak, J. B.; Hu, J. H.; Abbatt, J. P. D. *J. Geophys. Res.* **1997**, *102*, 18843.
(95) Cziczo, D. J.; Abbatt, J. P. D. *J. Phys. Chem. A* **2000**, *104*, 2038.
(96) Koop, T.; Kapilashrami, A.; Molina, L. T.; Molina, M. J. *J. Geophys. Res.* In press.
(97) Yoshitake, H. *Atmos. Environ.* **2000**, *34*, 2571.
(98) Rowland, B.; Kadagathur, N. S.; Devlin, J. P. *J. Chem. Phys.* **1995**, *102*, 13.
(99) Hemminger, J. C. *Int. Rev. Phys. Chem.* **1999**, *18*, 387.
(100) Masel, R. I. *Principles of Adsorption and Reaction on Solid Surfaces*; John Wiley & Sons: New York, 1996.
(101) Hucher, M.; Oberlin, A.; Hocart, R. *Bull. Soc. Fr. Mineral. Cristallogr.* **1967**, *90*, 320.
(102) Dai, Q.; Hu, J.; Salmeron, M. *J. Phys. Chem. B* **1997**, *101*, 1994.
(103) Luna, M.; Rieutord, F.; Melman, N. A.; Dai, Q.; Salmeron, M. *J. Phys. Chem. A* **1998**, *102*, 6793.
(104) Shindo, H.; Ohashi, M.; Baba, K.; Seo, A. *Surf. Sci.* **1996**, *357/358*, 111.
(105) Shindo, H.; Ohashi, M.; Tateishi, O.; Seo, A. *J. Chem. Soc., Faraday Trans.* **1997**, *93*, 1169.
(106) Otterson, D. A. *J. Chem. Phys.* **1963**, *38*, 1481.
(107) Lad, R. A. *Surf. Sci.* **1968**, *12*, 37.
(108) Estel, J.; Hoinkes, H.; Kaarmann, H.; Nahr, H.; Wilsch, H. *Surf. Sci.* **1976**, *54*, 393.
(109) Folsch, S.; Henzler, M. *Surf. Sci.* **1991**, *247*, 269.
(110) Dai, D. J.; Peters, S. J.; Ewing, G. E. *J. Phys. Chem.* **1995**, *99*, 10299.
(111) Allouche, A. *J. Phys. Chem. B* **1998**, *102*, 10223.
(112) Ahlswede, B.; Jug, K. *Surf. Sci.* **1999**, *439*, 86.
(113) Folsch, S.; Stock, A.; Henzler, M. *Surf. Sci.* **1992**, *264*, 65.
(114) Wassermann, B.; Mirbt, S.; Reif, J.; Zink, J. C.; Matthias, S. *J. Chem. Phys.* **1993**, *98*, 10049.
(115) Bruch, L. W.; Glebov, A.; Toennies, J. P.; Weiss, H. *J. Chem. Phys.* **1995**, *103*, 5109.
(116) Barraclough, P. B.; Hall, P. G. *Surf. Sci.* **1974**, *46*, 393.
(117) Smart, R. S. C.; Sheppard, N. *J. Chem. Soc., Faraday Trans. 2* **1976**, *72*, 707.
(118) Peters, S. J.; Ewing, G. E. *Langmuir* **1997**, *13*, 6345.
(119) Peters, S. J.; Ewing, G. E. *J. Phys. Chem. B* **1997**, *101*, 10880.
(120) Weis, D. D.; Ewing, G. E. *J. Geophys. Res.* **1999**, *104*, 21.
(121) Foster, M.; Ewing, G. E. *Surf. Sci.* **1999**, *428*, 102.
(122) Foster, M. C.; Ewing, G. E. *J. Chem. Phys.* **2000**, *112*, 6817.
(123) Brimblecombe, P.; Clegg, S. L. *J. Atmos. Chem.* **1988**, *7*, 1.
(124) Clegg, S. L.; Brimblecombe, P. *J. Phys. Chem.* **1990**, *94*, 5369.
(125) Tang, I. N.; Munklewitz, H. R.; Lee, J. H. *Atmos. Environ.* **1988**, *22*, 2579.
(126) Leu, M.-T.; Timonen, R. S.; Keyser, L. F.; Yung, Y. L. *J. Phys. Chem.* **1995**, *99*, 13203.
(127) Kester, D. R.; Duedall, I. W.; Connors, D. N.; Pytkowicz, R. M. *Limnol. Oceanogr.* **1967**, *12*, 176.
(128) Gebel, M. E.; Finlayson-Pitts, B. J.; Ganske, J. S. *Geophys. Res. Lett.* **2000**, *27*, 887.
(129) Kolb, C. E.; Worsnop, D. R.; Zahniser, M. S.; Davidovits, P.; Keyser, L. F.; Leu, M.-T.; Molina, M. J.; Hanson, D. R.; Ravishankara, A. R.; Williams, L. R.; Tolbert, M. A. Laboratory Studies of Atmospheric Heterogeneous Chemistry. In *Progress and Problems in Atmospheric Chemistry*; Barker, J. R., Ed.; World Scientific: Singapore, 1995; Vol. 3; pp Ch. 18.
(130) Kolb, C. E.; Jayne, J. T.; Worsnop, D. R.; Davidovits, P. **1997**, *69*, 959.
(131) DeHaan, D. O.; Finlayson-Pitts, B. J. *J. Phys. Chem. A* **1997**, *101*, 9993.
(132) Langer, S.; Pemberton, R. S.; Finlayson-Pitts, B. J. *J. Phys. Chem. A* **1997**, *101*, 1277.
(133) DeHaan, D. O.; Brauers, T.; Oums, K.; Stutz, J.; Nordmeyer, T.; Finlayson-Pitts, B. J. *Int. Rev. Phys. Chem.* **1999**, *18*, 343.
(134) Jayson, G. G.; Parsons, B. J.; Swallow, A. J. *J. Chem. Soc., Faraday Trans. 1* **1973**, *69*, 1597.
(135) Singh, H. B.; Kasting, J. F. *J. Atmos. Chem.* **1988**, *7*, 261.
(136) Knipping, E. M.; Lakin, M. J.; Foster, K. L.; Jungwirth, P.; Tobias, D. J.; Gerber, R. B.; Dabdub, D.; Finlayson-Pitts, B. J. *Science* **2000**, *288*, 301.

(137) Pearlman, D. A.; Case, D. A.; Caldwell, J. W.; Ross, W. S.; Cheatham, T. E.; DeBolt, S. E.; Ferguson, D. M.; Seibel, G. L.; Kollman, P. A. *Comput. Phys. Commun.* **1995**, *91*, 1.

(138) Essmann, U.; Perera, L.; Berkowitz, M. L.; Darden, T.; Pedersen, L. G. *J. Chem. Phys.* **1995**, *103*, 8577.

(139) Stuart, S. J.; Berne, B. J. *J. Phys. Chem.* **1996**, *100*, 11934.

(140) Stuart, S. J.; Berne, B. J. *J. Phys. Chem.* **1999**, *103*, 10300.

(141) Jacobi, H. W.; Wicktor, F.; Herrmann, H.; Zellner, R. *Int. J. Chem. Kinet.* **1999**, *31*, 169.

(142) Jungwirth, P., personal communication, 2000.

(143) Hopper, J. F.; Barrie, L. A.; Silis, A.; Hart, W.; Gallant, A. J.; Dryfout, H. *J. Geophys. Res.* **1998**, *103*, 1481.

(144) Taube, H. *J. Am. Chem. Soc.* **1942**, *64*, 2468.

(145) Haag, W. R.; Hoigne, J. *Environ. Sci. Technol.* **1983**, *17*, 261.

(146) von Gunten, U.; Hoigne, J. *Environ. Sci. Technol.* **1994**, *28*, 1234.

(147) Eigen, M.; Kustin, K. *J. Am. Chem. Soc.* **1962**, *84*, 1355.

(148) Abbatt, J. P. D. *Geophys. Res. Lett.* **1994**, *21*, 665.

(149) Kirchner, U.; Benter, T.; Schindler, R. N. *Ber. Bunsen-Ges. Phys. Chem.* **1997**, *101*, 975.

(150) Allanic, A.; Oppliger, R.; Rossi, M. J. *J. Geophys. Res.* **1997**, *102*, 23529.

(151) Mochida, M.; Akimoto, H.; vanDenBergh, H.; Rossi, M. J. *J. Phys. Chem. A.* **1998**, *102*, 4819.

(152) Fickert, S.; Adams, J. W.; Crowley, J. N. *J. Geophys. Res.* **1999**, *104*, 23719.

(153) Wang, T. X.; Margerum, D. W. *Inorg. Chem.* **1994**, *33*, 1050.

(154) Bartlett, W. P.; Margerum, D. W. *Environ. Sci. Technol.* **1999**, *33*, 3410.

(155) Foster, K. L.; Plastridge, R. A.; Bottenheim, J. W.; Shepson, P. B.; Finlayson-Pitts, B. J.; Spicer, C. W. *Science* **2000**, submitted for publication.

(156) Ellison, G. B.; Tuck, A. F.; Vaida, V. *J. Geophys. Res.* **1999**, *104*, 11633.

(157) Gill, P. S.; Graedel, T. E.; Weschler, C. J. *Rev. Geophys. Space Phys.* **1983**, *21*, 903.

(158) Andrews, E.; Larson, S. M. *Environ. Sci. Technol.* **1993**, *27*, 857.

(159) Wagner, J.; Andrews, E.; Larson, S. M. *J. Geophys. Res.* **1996**, *101*, 19533.

(160) Hansson, H. C.; Wiedensohler, A.; Rood, M. J.; Covert, D. S. *J. Aerosol Sci.* **1990**, *21*, S241.

(161) Hameri, K.; Rood, M. J.; Hansson, H. C. **1992**, *23*, Suppl. 1, S437.

(162) Thomas, E.; Trakhtenberg, S.; Ussyshkin, R.; Rudich, Y. *J. Geophys. Res.* **1999**, *104*, 16053.

(163) Rudich, Y.; Benjamin, I.; Naaman, R.; Thomas, E.; Trakhtenberg, S.; Ussyshkin, R. *J. Phys. Chem. A* **2000**, *104*, 5238.

(164) Lai, C. C.; Yang, S.; Finlayson-Pitts, B. J. *Langmuir* **1994**, *10*, 4637.

(165) Wadia, Y.; Tobias, D. J.; Stafford, R.; Finlayson-Pitts, B. J. *Langmuir*, in press.

(166) Moise, T.; Rudich, Y. *J. Geophys. Res.* **2000**, *105*, 14667.

(167) Ghosal, S.; Shbeeb, A.; Hemminger, J. C. *Geophys Res. Lett.* **2000**, *27*, 1879.

(168) Seisel, S.; Caloz, F.; Fenter, F. F.; van den Bergh, H.; Rossi, M. J. *Geophys. Res. Lett.* **1997**, *24*, 2757.

(169) Seisel, S.; Fluckiger, B.; Caloz, F.; Rossi, M. J. *Phys. Chem. Chem. Phys.* **1999**, *1*, 2257.

(170) Caloz, F.; Seisel, S.; Fenter, F. F.; Rossi, M. J. *J. Phys. Chem. A* **1998**, *102*, 7470.

(171) Caloz, F.; Fenter, F. F.; Tabor, K. D.; Rossi, M. J. *Rev. Sci. Instrum.* **1997**, *68*, 3172.